Translated from *Uspekhi Khimii* **59** 1179–1212 (1990) U.D.C. 548.737

The structure of novel conductive dithiolate complexes

V E Shklover, S S Nagapetyan, Yu T Struchkov
Nesmeyanov Institute of Organoelemental Compounds, USSR Academy of Sciences, Moscow

ABSTRACT. The characteristics of the molecular and crystalline structure of novel transition metal dithiolate complexes are examined and the correlation between structure and electrical conductivity of these compounds is discussed. The material reviewed is of interest both for the crystal chemistry and physical chemistry of the respective class of molecular conductors and for the structural chemistry of dithiolates.

The bibliography includes 94 references.

Contents

I. Introduction 686
II. Structure of salts of 4,5-dimercapto-2-thione-1,3-dithiolates with "closed" cations 687
III. Structure of salts of 4,5-dimercapto-2-thione-1,3-dithiolates with "open" cations 695
IV. Crystalline structures of 5,6-dihydro-1,4-dithiin-2,3-dithiolate complexes and their salts 700
V. Conclusion 704

I. Introduction

Solid-state reactions are of increasing interest to research workers. This is because the limited mobility of reacting molecules in a crystal makes it possible to carry out a successive structural study of a whole chain of molecular reactions and to obtain polymers of a regular structure, large, defect-free monocrystals, etc. This is all due to the origination and development of a new branch of science—crystal engineering—which is aimed at studying the principles and laws governing the formation of those types of packing of potentially reactive molecules and crystals in which favourable conditions are created for the molecules to participate in given reactions and rearrangements.[1–21]

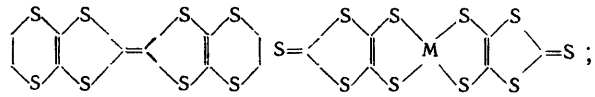
At the present time the concepts of crystal engineering have been developed further in studies on crystalline low-dimensional semiconductors, metals, and superconductors. Special emphasis has been given to research on the properties of this promising class of organic materials (the design of molecular "corridors" of the primary movement of electrons, the use of heteroatoms for achieving overlap of orbitals of neighbouring molecules, the elimination of spatial modulation of charge density by changing the intermolecular distances, etc.).

The structure and packing of donor and acceptor molecules in crystals of organic conductors have a number of specific features. Donor molecules should be planar and include π-residues and heteroatoms (nitrogen, oxygen, or chalcogen atoms). For acceptor molecules the shape, size, and charge are important. In the crystal the donor and acceptor molecules should be located so as to achieve the necessary electronic interaction for delocalisation of electrons and high electrical conductivity. In other words, the molecular building blocks of an organic conductor should be well suited to achieve overlap between the π-electron systems of neighbouring molecules. By changing the structure of donor and acceptor molecules and also the conditions for obtaining the organic conductor that affect its composition (the ratio of donor to acceptor), it is possible to vary the crystalline structure, and this in turn leads to a change in the degree of charge transfer and electrical conductivity of the crystal under these conditions. As examples of the "active" modification of the properties of an organic metal (or superconductor) through alteration of the molecular structure of its components, mention can be made, for example, of the change from salts of the type TTF–TCNQ to the salts $(TMTSF)_2X$ (for notation see Table 1), the structure of which exhibits more pronounced two-dimensional characteristics as a result of introducing Me groups and Se atoms into the donor molecule and replacing acceptors of the type TCNQ by monovalent anions of the type X = PF_6;[22–24] the change from salts of the type $(TMTSF)_2X$ to salts of the type $(BEDT-TTF)_2Y_3$, which have a stronger interstack interaction and a higher value of the transition temperature to a superconductive state (T_c) as a result of replacement of the donors TMTSF by BEDT–TTF;[25–27] and the further increase in T_c in $(BEDT-TTF)_2Y_3$ salts by altering the Y_3 anions ("chemical compression" effect).[28–31]

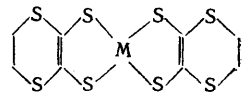
At the present time organic metals and superconductors in which BEDT–TTF acts as the donor have been studied the most actively. In contrast to conductive radical cation salts with packing in stacks (perylenium salts, for example),[32] in crystals of BEDT–TTF salts the central π-electron system of the molecule† is not involved in intermolecular interaction. On the other hand, in conductive crystals, the so-called one-dimensional transition metal complexes with organic ligands, the conductive corridors are in fact produced from the electrons of the "central" metal ions interacting with their neighbours in the stack situated above and below the central ion. The organic ligands do not participate in intermolecular electron transfer.[33] It was natural that the idea of synthesising compounds that would simultaneously combine the properties of salts of the type BEDT–TTF and those of one-dimensional metal complexes should develop (see, for example, the study of Keller et al.),[34] and this was carried out at approximately the same time by different groups of research workers. They synthesised transition metal complexes with novel sulphur-containing ligands such as $[M(dmit)_2]^n$ and

†In this and other cases (which will subsequently not be mentioned separately) we are, of course, dealing with a radical ion (in this case the radical cation $BEDT-TTF^{+\cdot}$) that is called a "molecule" in order to simplify the discussion of the crystalline structure in terms of the crystal chemistry of molecular crystals.

$[M(DDDT)_2]^n$. Their salts have a close structural similarity to salts of BEDT–TTF.



BEDT—TTF $[M(dmit)_2]^n$



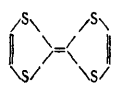
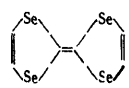
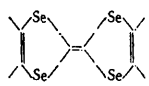
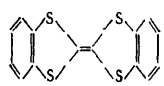
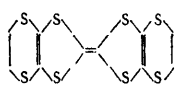
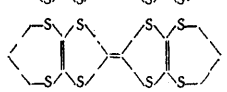
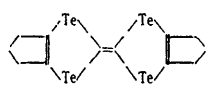
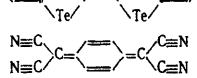
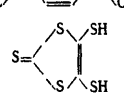
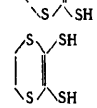
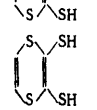
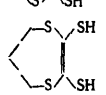
$[M(DDDT)_2]^n$

The complexes $[M(dmit)_2]^n$ and $[M(DDDT)_2]^n$ belong to a well-known class of dithiolate complexes. The structure of simpler dithiolate complexes has been discussed several times (see, for example, two studies[35,36]). Thus, their molecules or ions were observed to have an overall planar structure regardless of the nature of metal or its degree of oxidation, a capacity for reversible electron transfer reactions with the formation of stable products, considerable delocalisation of the π-type HOMO, and a high electron-acceptor capacity relative to organic donors.

Dithiolate complexes have considerable structural flexibility (geometric and electronic) with regard to replacement of the central metal atom and the substituents in the ligands and counterions.

In this review the literature data and the present authors' own results in studies on the structure of novel sulphur-containing dithiolate complexes of the type $[M(dmit)_2]^n$ and $[M(DDDT)_2]^n$ and on the search for correlations between structure and electrical conductivity are examined.

Table 1. Notation used in this review.

Name	Structural formula	Notation
Tetrathiafulvalene		TTF
Tetraselenafulvalene		TSF
Tetramethyltetraselenafulvalene		TMTSF
Dibenzotetrathiafulvalene		DBTTF
Bis(ethylenedithio)tetrathia-fulvalene		BEDT—TTF
Bis(propylenedithio)tetrathia-fulvalene		BPDT—TTF
Bis(trimethylene)tetratellura-fulvalene		HMTTeF
Tetracyanoquinodimethane		TCNQ
4,5-Dimercapto-1,3-dithiole-2-thione		H_2dmit
5,6-Dihydro-1,4-dithiin-2,3-dithiol		H_2DDDT
1,4-Dithiin-2,3-dithiol		H_2DDT
5,6-Dihydro-1,4-dithiepin-2,3-dithiol		H_2DDTDT

II. Structure of salts of 4,5-dimercapto-2-thione-1,3-dithiolates with "closed" cations

Table 2 lists the main data on the structures and conductivity of $Cat_x[M(dmit)_2]^{x-}$ salts, formed with "closed" cations. These are cations of the type Me_4N^+, Et_4N^+, Me_3S^+, Ph_4As^+, etc., which, in contrast to cations (donors) of the type TTF, TMTSF, and BEDT–TTF, are incapable of intermolecular electron transfer. Since in all cases Cat is a single-charged cation, the value of x is equal to the formal average negative charge of the complex anion $[M(dmit)_2]^{x-}$. In the crystal of the neutral complex $Ni(dmit)_2$ (I)[37] the molecules are arranged in a displaced manner in stacks, the normal to the plane of the complex forms an angle of 48.0° with the [010] direction. There is one shortened intermolecular S...S contact (3.577 Å) within a stack and three contacts between stacks (3.580, 3.580 and 3.575 Å). In the opinion of Valade et al.,[37] the interstack contacts have a short length because they are formed by the thione S atoms and the corresponding S...S vectors are aligned at considerable angles to the plane of complex (I) (far from parallel to this plane).‡ In other words, because of the anisotropy in the relative orientation of the π-atomic orbitals of the atoms in different molecules, even close contacts can lead to small values of the electron hopping parameter.

It has been observed by Valade et al.[37] that the crystal of (I) meets the structural requirements needed for highly conductive systems (the occurrence of regular stacks and reduced intermolecular distances) but it does not satisfy the main electronic criterion—the occurrence of a fractional charge, which accounts for the low conductivity of (I) ($\sigma \sim 3.5 \times 10^{-3}$ Ω^{-1} cm^{-1}).§ Localisation of a

‡In an analysis of the crystalline structure of organic conductors, the interaction (orbital overlap) between neighbouring molecules is determined by comparing the intermolecular distances with the sum of the van der Waals radii of the atoms (see, for example, Pauling[51]). In molecular crystals at room temperature the orbital overlap is small if the intermolecular distances are greater than the sum of the van der Waals radii. At distances smaller than the sum of the van der Waals radii, the contribution of orbital overlap increases exponentially.[52] In addition to the absolute values of the intermolecular distances it is also necessary to take into account the relative orientation of the orbitals of the molecules in contact (see, for example, the study of Mori et al.[53]) in a determination of orbital overlap.

§The specific conductivity σ of insulators varies over the range $10^{-22}-10^{-15}$ Ω^{-1} cm^{-1}, for semiconductors it varies over the range $10^{-8}-10^{-2}$ Ω^{-1} cm^{-1} (increases as the temperature is increased), and for metals the variation is $10-10^4$ Ω^{-1} cm^{-1} (increases as the temperature is lowered).

Table 2. The main data on $Cat_x[M(dmit)_2]^{x-}$ compounds.

Compound	Chemical formula	Structural motif	d, Å*	M–S distances, Å	Conductivity σ_{293}, Ω^{-1} cm^{-1}	Refs.
(I)	$Ni(dmit)_2$	Stacks	3.56	2.147(2)	$3.5\cdot10^{-3}$	[37]
(II)	$(Me_4N)_{0.5}[Ni(dmit)_2]$	" Layers	3.53; 3.58	2.158	50	[38, 39]
(III)	α-$\{(Me_2Et_2N)_{0.5}[Ni(dmit)_2]\}$	Stacks Layers	3.52	see**	20–100	[40]
(IV)	$(Et_4N)_{0.5}[Ni(dmit)_2]$	Stacks Layers	3.44; 3.76	2.146–2.154(3)	$4.5\cdot10^{-2}$	[41]
(V)	$(Bu_4N)_{0.29}[Ni(dmit)_2]\cdot MeCN$	Stacks Layers	3.51–3.57	2.153(4)	1–10	[37, 42]
(VI)	$(Bu_4N)_2[Ni(dmit)_2]$	Not formed	—	2.211; 2.221(6)	see**	[43]
(VII)	$(Bu_3S)[Ni(dmit)_2]$	Dimers	3.63	2.161–2.174(2)	10^{-6}	[44]
(VIII)	$(Ph_4As)_{0.25}[Ni(dmit)_2]$	Stacks Layers	3.50–3.61	2.152–2.171(6)	10–15	[45]
(IX)	$(Bu_4N)[Pt(dmit)_2]$	Chains	—	see**	$<10^{-8}$	[46]
(X)	α-$\{(Et_4N)_{0.5}[Au(dmit)_2]\}$ [isostructural to (IV)]	Stacks Layers	3.79; 3.49	2.314–2.321(1)]	0.2	[47]
(XI)	$(Et_4N)[Au(dmit)_2]$	Stacks	3.64; 3.57	2.311–2.320(2)	10^{-5}	[48]
(XII)	$(Bu_4N)[Au(dmit)_2]$	Chains	—	2.316–2.327(4)	see**	[49]
(XIII)	$(Me_3S)[Au(dmit)_2]$	Thin layers	3.59	2.307–2.323(3)	10^{-5}	[50]
(XIV)	$(Bu_3S)[Au(dmit)_2]$ [isostructural to (VII)]	Dimers	3.67	2.304–2.319(2)	10^{-6}	[44]

*Interplanar distance (between planes of neighbouring anions in a stack or between planes of layers) is given.
**These figures were not given in the original study.
***Insulator.

fractional charge on donor and acceptor molecules in the crystal of an organic metal assists the formation of vacancies on to which electrons can hop at sufficiently high values of the resonance parameters.

In the crystal of $(Me_4N)_{0.5}[Ni(dmit)_2]$ (II) the almost planar $[Ni(dmit)_2]^{1/2-}$ complexes are stacked along the [110] direction. The distances between the planes of the complexes in the stacks alternate between 3.53 and 3.58 Å (Fig. 1). The reduced intermolecular S...S contacts combine the stacks of anions into layers parallel to the (001) plane and alternating along the [001] direction) with layers of Me_4N^+ cations.

The electrical conductivity of the crystal of (II) in a plane parallel to the planes of the layers [parallel to the (001) plane of the crystal] is $\sim 50\ \Omega^{-1}$ cm^{-1} at room temperature, while in a plane perpendicular to the (001) plane it is $\sim 10^{-2}\ \Omega^{-1}$ cm^{-1}. At 100 K the crystal of (II) undergoes a metal–semimetal transition (concentration of conducting electrons decreases to $10^{-3}-10^{-5}$ electrons per atom) and the electrical conductivity along the planes of the layers falls to $1.4\times10^{-2}\ \Omega^{-1}$ cm^{-1}, with the resistance in the plane perpendicular to the layers remaining approximately 10^3 times higher in value.

The stacks of anions directed along [110] and [1$\bar{1}$0] alternate in the [001] direction. Significant is the absence of satellite reflections on the X-ray photographs of samples of (II) when they are cooled below 100 K, where the crystal of (II) undergoes a metal–semimetal transition. X-Ray diffraction analysis of a sample of (II) carried out at temperatures above (293 K) and below (92 K) the transition temperature did not reveal any structural differences in the crystal on changing the temperature.

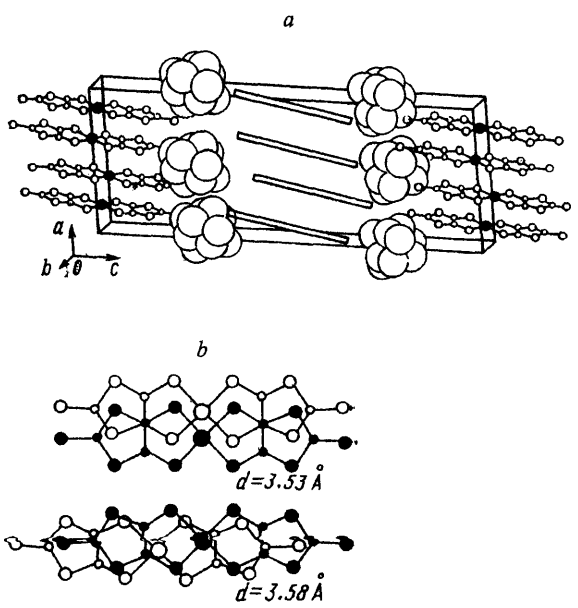


Figure 1. The structure of crystals of $(Me_4N)_{0.5}[Ni(dmit)_2]$ (II) at 95 K (*a*) and the two ways in which the $[Ni(dmit)_2]^{1/2-}$ anions are superimposed in stacks along the [110] direction[38,39] (*b*). The van der Waals spheres of the H atoms in the disordered Me_4N^+ cations are depicted as large circles. The anions perpendicular to the plane of Fig. 1 are shown as rods.

The dependence of the resistance of the crystal of (II) on pressure was studied up to a pressure of 7 kbar. On increasing the pressure the metal–semimetal transition is suppressed and above 3 kbar phenomena characteristic of a superconductive transition occur. At 7 kbar the transition temperature (T_c) was 5 K and the value of dT_c/dP for complex (II) was greater than zero. A positive value of dT_c/dP also occurs for $(TTF)_{0.5}[Ni(dmit)_2]$,[38,39] while for the salts $(TMTSF)_2X$ (X = ClO_4, PF_6, and others)[54] and β-(BEDT–TTF)$_2$X (X = I_3, IBr_2)[55] this value is less than zero.

The hysteresis from continuous heating and cooling a crystal of (II) over the range from about 90 to 300 K is attributed by Kobayashi et al.[39] to the rotational randomisation of the Me groups at room temperature, frozen out on cooling the samples to 95 K.

Compound (II) is the first molecular superconductor to consist of π-acceptor molecules and cations of a closed type.[39] Molecular superconductors consisting of π-donor molecules and closed anions [for example, Bechgaard salts $(TMTSF)_2X$] have previously been reported.[22–24]

In the crystal of α-{$(Me_2Et_2N)_{0.5}[Ni(dmit)_2]$} (III), obtained by electrochemical oxidation of the salt $(Me_2Et_2N)[Ni(dmit)_2]$, the planar $Ni(dmit)_2$ anions are arranged along the *b* axis in stacks in which two types of orbital overlap occur (Fig. 2) through intermolecular S...S contacts (3.424–3.605 Å). Overlap of type (A) occurs between a reference $Ni(dmit)_2$ molecule and two molecules that are not completely parallel to it (dihedral angle 171°), located above the reference one on the *b* axis (lapped overlap). Overlap of type (A) leads to the stacks being combined into layers. Overlap of type (B) takes place between a reference molecule and a molecule parallel to it which is located below on the *b* axis (interplanar distance *d* = 3.52 Å). In a crystal of (III) there are also very short intermolecular S...S distances (3.352 Å) between the thione S atoms of molecules in different layers along the *a* axis.

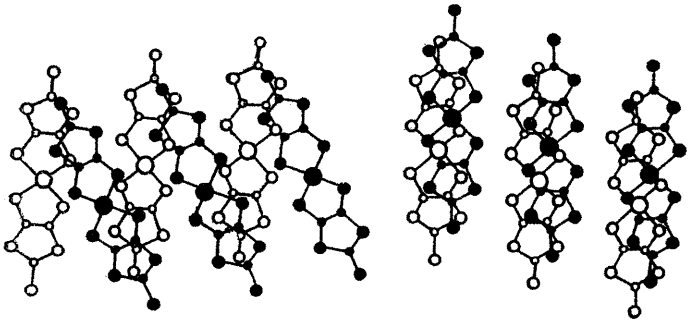


Figure 2. The two ways (*A* and *B*) in which the $[Ni(dmit)_2]^{1/2-}$ anions are superimposed in the crystal of (III).[40]

The electrical conductivity of crystals of (III) in the *bc* plane is isotropic, where σ_{293} = 20–100 Ω^{-1} cm^{-1}; this type of electrical conductivity (typical for metals) is retained down to 1.5 K and a metal–insulator transition does not occur. The electrical conductivity of crystals of (III) along the *a* axis is also quite high: σ_{293} = 1 Ω^{-1} cm^{-1}. At 1.5 K a superconductive transition occurs. Calculation of the overlap integrals of the LUMOs forming the conductivity zone using the extended Hückel (EH) method confirmed the essentially two-dimensional nature of the zone structure in crystals of (III). However, crystals of (III) differ from other $Cat_x[M(dmit)_2]^x$ salts in that for the first time a clear but small interaction was also observed in them in a "third" direction (along the *a* axis).

According to calculations[56] of the intermolecular overlap integrals of the LUMOs in crystals of a number of salts of $M(dmit)_2$ complexes it was found that the b_{2g} symmetry characteristic of these orbitals is not conducive for their overlap in the direction of the short axes of the planar molecules, which is not consistent with the formation of two-dimensional conductive motifs. However, the "lapped" overlap occurring in the crystal of (III) may be regarded as one of the ways of forming two-dimensional motifs.

In the crystal of (IV), which contains the larger Et_4N^+ cations, the $[Ni(dmit)_2]^{1/2-}$ anions are stacked along the [010] direction (Fig. 3).[41] In the stacks there are shortened intermolecular distances between molecules A and B′ but not between molecules A and B. The corresponding interplanar distances are equal to 3.437 Å (between A and B′) and 3.759 Å (between A and B), namely, the anion stacks consist of weakly bound dimers. There are a large number of shortened intermolecular S...S distances between the stacks of anions, as a result of which layers of interacting anions are formed parallel to the (100) plane in the crystal of (IV).

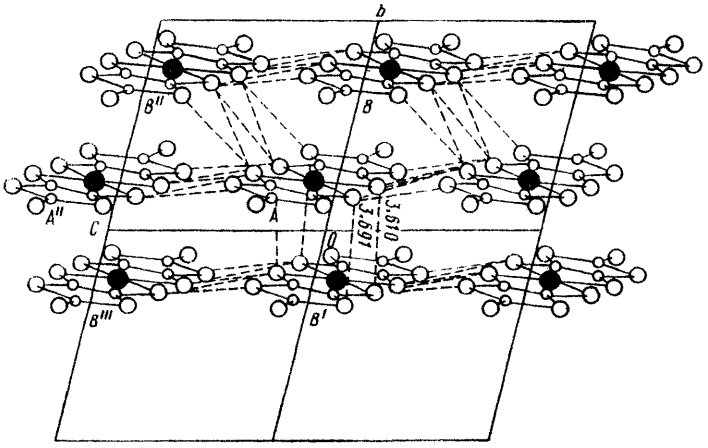


Figure 3. Projection of the crystalline structure of $(Et_4N)_{0.5}[Ni(dmit)_2]$ (IV) on to the *bc* plane (the Et_4N^+ cations are not shown).[41] Here and subsequently shortened intermolecular S...S contacts are indicated by broken lines.

It should be noted that the shortest S...S contacts occur between the "inner" S atoms of the $[Ni(dmit)_2]^{1/2-}$ complexes (3.499 Å), whereas the distances between the "outer" S atoms are more than twice the van der Waals radius of the S atom. Thus, the inner S atoms of the $[Ni(dmit)_2]^{1/2-}$ complexes play a more important role in interstack contacts.

The $[M(dmit)_2]^{x-}$ anions (*x* = 0, ... 1) in crystals of (I)–(VIII) are virtually planar. The bond lengths in the chelate centres of dithiolene complexes of transition metals vary according to their degree of oxidation.[41] The Ni–S distance [2.147(2) Å] in (I) is at the lower limit of the range of Ni–S distances in complexes (I)–(VIII). When the negative charge of the $[Ni(dmit)_2]^{x-}$ complex

is increased, in general there is a tendency for the Ni–S distances to increase (see Table 2). In both the neutral complex (I) and the negatively charged complex (IV) (x = ½), delocalisation of electron density through the chelate residues of the type (Ni)S⋯C⋯C⋯S(Ni) is substantial; the C=C bond lengths are increased to 1.391(9) Å in a crystal of (I) and to 1.39(1) and 1.40(1) Å in (IV), and the (Ni)S–C bond is shortened to 1.699(7) Å in (I) and to 1.682–1.701(7) Å in (IV) compared to the (S=C)S–C bonds in (I) [1.731(7) Å] and in (IV) [1.725–1.732(7) Å]. In the different salts of the anionic $[M(dmit)_2]^{x-}$ complexes the degree of delocalisation through the chelate residues of dithiolene complexes is apparent to a different extent (see below).

The crystal of (IV) is a semiconductor with a low anisotropy of conductivity. The maximum value of electrical conductivity occurs in the plane of the *ac* layer along the stacks ($\sigma_b = 4.5 \times 10^{-2}$ Ω^{-1} cm^{-1}), the energy of activation of electrical conductivity along the *a*, *b*, and *c* axes is 0.15, 0.16, and 0.16 eV respectively. At 300 K $\sigma_a:\sigma_b:\sigma_c = 1:50:8$.

The intermolecular overlap integrals (S) of the LUMOs of neutral $Ni(dmit)_2$ molecules placed in the positions occupied by the corresponding anions in the crystal of (IV) have been calculated using the extended Hückel method. The values of S for the molecules within the stacks [S(A–B′) = 9.06×10^{-3}, S(A–B) = -2.06×10^{-3}] are higher than those between stacks [S(A–A″) = 1.17×10^{-3}, S(A–B″) = 0.89×10^{-3}, S(A–B‴) = 0.27×10^{-3}], which is consistent with the direction of maximum electrical conductivity.

The crystal of $(Bu_4N)_{0.29}[Ni(dmit)_2]$.MeCN (V) contains eight crystallographically independent $[Ni(dmit)_2]^{0.29-}$ anions (j = 1–8), two of which (j = 1 and 5) are located at centres of symmetry, two crystallographically independent Bu_4N^+ cations, and two MeCN solvate molecules. In all of the (Ni)S⋯C⋯C⋯S(Ni) chelate residues conjugation is clearly apparent—the C=C, (Ni)S–C, and (S=C)S–C distances are (on average) equal to 1.39(2), 1.70(2), and 1.74(2) Å respectively.

The $[Ni(dmit)_2]^{0.29-}$ anions are arranged along the [110] direction into stacks of two types (Fig. 4). In the stacks centrosymmetric triads and tetrads of complexes alternate. The axes of the triads and tetrads are parallel and form angles of ~21° with the plane of the [110] stack. The distances between the mean planes of the complexes in the stacks, which vary from 3.48 to 3.57 Å, are typical for a strong intermolecular π-interaction; for example, in the crystal of (TTF)$[Ni(dmit)_2]_2$ (XV), which has the conductivity of a metal, the interplanar distance in a regular stack is 3.55 Å.[57] According to Soos et al.,[33] an irregular stack structure [both in terms of the interplanar distances (Fig. 4) and the nature of the molecular overlap] is probably responsible for the "nonmetallic" nature of the conductivity in the crystal of (V).

The large number of shortened interstack S...S contacts (34 of the 39 interanion S...S contacts, less than 3.60 Å, relate to contacts between stacks, the shortest of these contacts being 3.442 Å) combine the stacks of $Ni(dmit)_2$ complexes in the crystal of (V) into layers parallel to the (001) plane and separated by layers of Bu_4N^+ cations and MeCN solvate molecules.

Crystals of (V) have a thermally activated (E_a = 0.02–0.1 eV) electrical conductivity σ_{300} = 1–10 Ω^{-1} cm^{-1}. The weak electroconductive anisotropy observed ($\sigma_a/\sigma_b \approx 1$) is consistent with the two-dimensional nature of the structure of (V). The low electrical conductivity in the third direction (along the *c* axis, $\sigma_{300} \approx 10^{-3}$ Ω^{-1} cm^{-1}) is due to the presence of barrier layers of Bu_4N^+ cations and MeCN molecules parallel to the (001) plane.

The Ni–S distances [2.211 and 2.221(6) Å] in the $[Ni(dmit)_2]^{2-}$ anion of the crystal of (VI)[43] are greater than the distances that occur in the $[Ni(dmit)_2]^{x-}$ anions of other complexes (see Table 2) that have a lower negative charge. Information is available[43] on this type of relationship between the Ni–S distances and charges on the anions in simpler dithiolate Ni complexes. The (Ni)S–C distances in the crystal of (VI) [1.74 and 1.76(1) Å] are greater than the

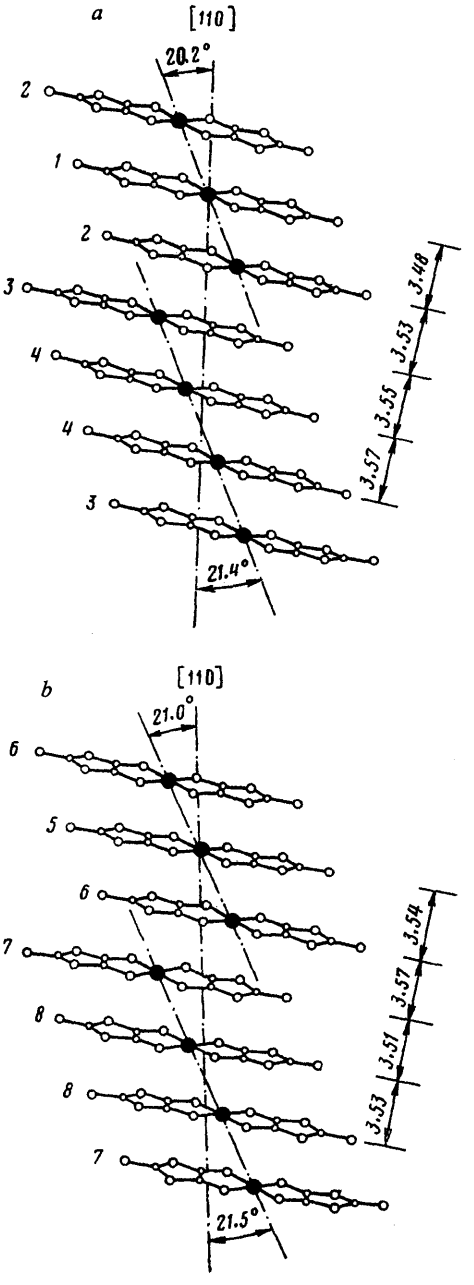


Figure 4. Packing of planar $Ni(dmit)_2$ complexes in the crystal of $(Bu_4N)_{0.29}[Ni(dmit)_2]$.MeCN (V) in stacks of two types (*a* and *b*) along the [110] direction. A projection on to the plane including the [110] vector and the long axis of the complex (the line joining the thione S atoms) is given.[37]

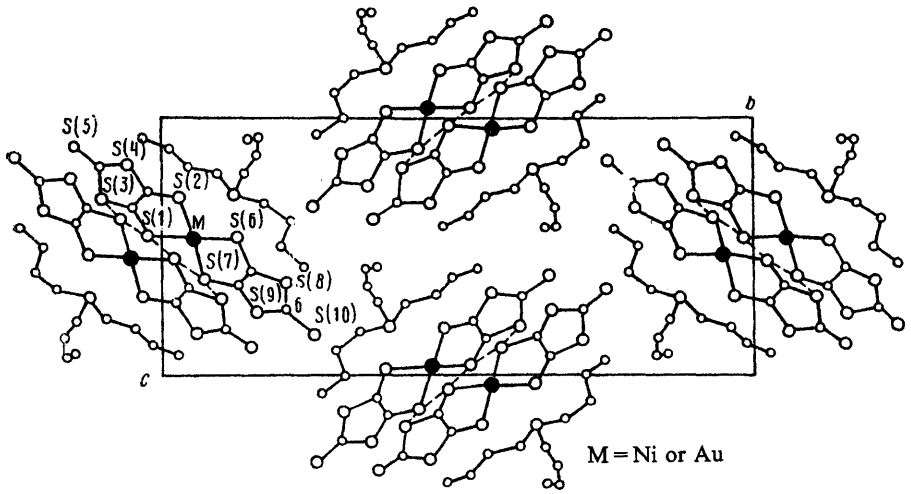


Figure 5. Projection of the isostructural crystals of $(Bu_3S)[Ni(dmit)_2]$ (VII) and $(Bu_3S)[Au(dmit)_2]$ (XIV) on to the *bc* plane.

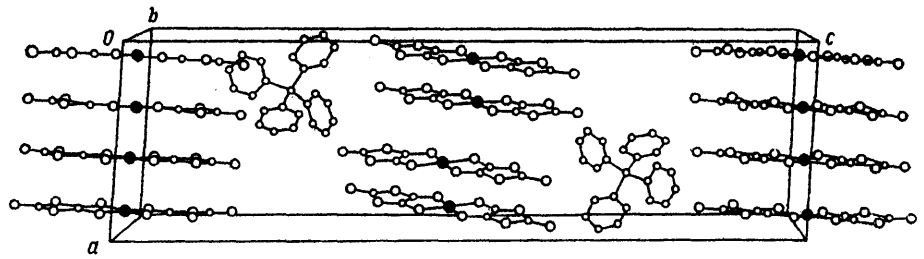


Figure 6. The crystalline structure of (VIII).[45]

(S=C)S−C distances [1.71 and 1.72(1) Å] and the C=C distance is somewhat increased [1.39(2) Å]. The anion of (VI) has an optimum planar structure and an actual optimum characteristic *mmm* symmetry. There are no characteristic structural motifs or shortened intermolecular contacts in the crystal of (VI).

Crystals of the insulator (VII) [and crystals of (XIV) which are isostructural to them] do not contain infinite structural motifs and they are composed of anions joined into dimers by (0, ½, ½) centres of symmetry (Fig. 5). In the dimers there are shortened S(1)...S(1′) contacts of 3.620(3) Å, S(1)...S(7′) contacts of 3.681(3) Å, and S(3)...S(7′) contacts of 3.605(3) Å between $[Ni(dmit)_2]^-$ anions, while in the dimers of the crystal of (XIV), where the $[Au(dmit)_2]^-$ anions are packed more closely than in the Ni analogue, these S...S contacts are 3.496, 3.491, and 3.551(3) Å. The somewhat greater degree of flattening of $[Au(dmit)_2]^-$ anions in (XIV) compared to $[Ni(dmit)_2]^-$ anions in (VII) may also be mentioned (the maximum deviation of the atoms in the anion from its mean plane is given by Δ_{max} = 0.073 and 0.102 Å respectively).

The crystal of (VIII) is composed of two independent $[Ni(dmit)_2]^{0.25-}$ anions in general positions and a Ph_4As^+ cation occupying an individual position on axis 2. The structure of the crystal of (VIII) may be described as consisting of layers of $[Ni(dmit)_2]^{0.25-}$ complexes parallel to the (001) plane, separated by layers of Ph_4As^+ cations (Fig. 6). In the anion layers stacks are formed along the $[\bar{1}10]$ direction when $z \approx 0$ and [110] direction when $z \approx ½$. The stacks consist of approximately parallel complexes grouped into tetrads (Fig. 7). The intermolecular distances in the tetrads (3.53, 3.50, and 3.53 Å) are in good agreement with the observed interplanar distance of 3.55 Å in regular stacks of the crystal of $(TTF)[Ni(dmit)_2]_2$ (XV), which is electroconductive at a low temperature.[57,58] The interplanar distance of d = 3.61 Å between the tetrads is appreciably greater than within the tetrads and is an indication of the "modulated" structure of the stacks.¶ A modulated arrangement of the planar anions in stacks also occurs in the related structures (IV) and (V)—alternation of the diads in (IV) and of the triads and tetrads in (V). Within the triads and tetrads the interplanar distances d vary from 3.48 to 3.57 Å while in the diads they are 3.44 Å. Judging by the interplanar distances, the $[Ni(dmit)_2]^{x-}$ anions interact more strongly within the diads [the crystal of (IV)] than within the triads and tetrads [crystals of (V) and (VIII)]. This is also supported by the distances between the diads, triads, and tetrads in the stacks; in (IV) the interplanar distance between diads is equal to 3.76 Å, in (V) the interplanar distance between triads is 3.53 Å and between tetrads is 3.57 Å, while in (VIII) the interplanar distance between tetrads is 3.61 Å.

¶The occurrence in the stack of two or more interplanar distances rather than one is implied.

The type of overlap of $[Ni(dmit)_2]^{0.25-}$ complexes in the tetrads of the crystal of (VIII) is shown in Fig. 8. It is clear that within the tetrads there is an appreciable relative lateral shift of the molecules, which leads to overlap of the complexes within the tetrads of the type "sulphur-over-ring" (Fig. 8*a*). Conversely, between the tetrads a longitudinal shift generally occurs, leading to overlap of the complexes of the type "metal-over-ring" (Fig. 8*b*), which may be regarded as a disturbance of the continuous structure of a stack.

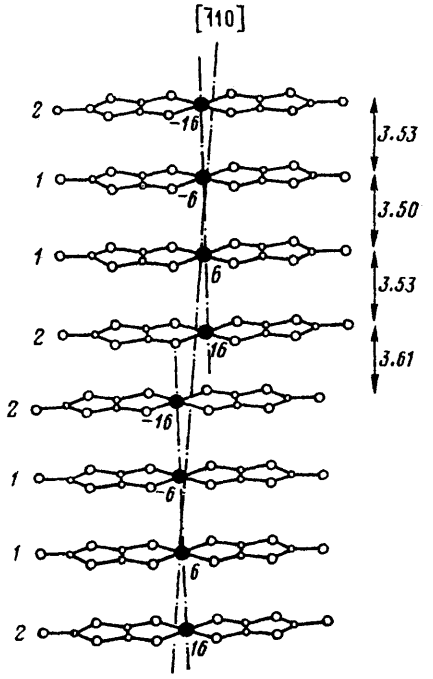


Figure 7. Projection of the anion stacks in the crystal of (VIII) on to the plane defined by the [$\bar{1}$10] vector and the long axis of the complex (the line joining the thione S atoms). The interplanar distances and magnitudes of projection of the Ni atoms from this plane ($\times 10^{-2}$ Å) are shown. The two symmetrically independent $Ni(dmit)_2$ complexes[45] are denoted by the numbers j = 1, 2.

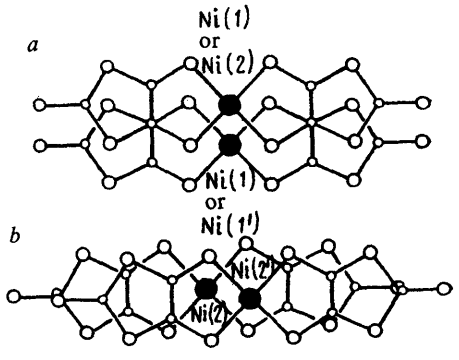


Figure 8. Intrastack overlap of $[Ni(dmit)_2]^{0.25-}$ complexes within the tetrads (*a*) and between the tetrads (*b*) of the crystal of (VIII).[45]

In the crystal of (VIII) almost all of the intermolecular S...S distances which are less than twice the van der Waals radius of the S atom (3.70 Å)[51] are contacts between stacks. If the limited disturbance to the regular stack structure (shifts of the molecules in the stacks in lateral and longitudinal directions) as mentioned above is neglected, the shortened interstack S...S contacts lead to the formation of layer motifs, parallel to the (001) plane, in the crystal of (VIII). The occurrence of these two-dimensional structural motifs governs the two-dimensional nature of the electroconductive properties of salt (VIII) [like salts (II)–(V)]. However, while the layers of Bu_4N^+ and Ph_4As^+ cations in (V), (VI), and (VIII) form "strong" barriers, virtually eliminating electrical conductivity in a "third" direction (perpendicular to the layers of $[Ni(dmit)_2]^{x-}$ anions), cations that are smaller in size, such as Et_4N^+ in (IV), also allow electrical conductivity in the third direction, resulting from the weak interaction between the terminal S atoms of neighbouring anion layers (the corresponding S...S distances are 3.90 Å). Thus, salt (IV) may be regarded as the precursor of a three-dimensional molecular metal.

It is likely that the tendency to form three-dimensional electroconductive motifs would be strengthened by replacing the Et_4N^+ cations with sulphur-containing cation-radical donor molecules.[44] In fact, in the crystal of $(TTF)_{0.5}[Ni(dmit)_2]$ the layers of $[Ni(dmit)_2]^{1/2-}$ complexes are combined with TTF molecules through S...S contacts into a quasi-three-dimensional structure.[58]

The electrical conductivity along the [010] direction of needle-shaped crystals of (VIII) is 10–15 Ω^{-1} cm^{-1}. This direction corresponds to the axis of the needles and is perpendicular to the most extensive plane of laminar crystals of (VIII). The electrical conductivity has a thermally activated nature. Low anisotropy of electrical conductivity in the (001) plane of the laminar crystal of (VIII) has been recorded ($\sigma_a : \sigma_b : \sigma_c = 1 : 1 : 10^{-5}$).

In contrast to salts (I)–(VIII), there are no anion stacks in the crystal of $(Bu_4N)[Pt(dmit)_2]$ (IX) but chains along the c axis can be distinguished, formed through interanion S...S contacts (3.55 Å). There are not enough of these contacts to form an electroconductive system; electrical conductivity along the chain is given by $\sigma_c < 10^{-8}$ Ω^{-1} cm^{-1}. The low electrical conductivity of crystals of (IX) is consistent with its IR spectrum; in the region of 400–4000 cm^{-1} there is no broad band characteristic of highly conductive molecular complexes.[46] It follows from the EPR spectra that the unpaired electrons in $[Pt(dmit)_2]^-$ anions are located on the Pt atoms.[46] Measurement of the temperature dependence of magnetic susceptibility indicates that indirect antiferromagnetic exchange through the system of these intermolecular S...S contacts occurs in the crystal of (IX).

The question of the similarity in crystal structure of the semiconductor (X) and its precursor (XI) [compound (X) is obtained by oxidation of salt (XI)], which is an insulator, is of interest. The $[Au(dmit)_2]^{x-}$ anions in crystals of (X) and (XI) retain an approximately planar structure [Δ_{max} = 0.048 Å in (X) and 0.13 Å in (XI)], the Au–S and C=C bond lengths in (X) and (XI) are similar [Au–S is 2.314–2.321(1) Å and C=C is 1.349 and 1.351(6) Å in (X) and Au–S is 2.311–2.320(2) Å and C=C is 1.345 and 1.365(9) Å in (XI)]. In (X), however, there is a difference between the (Au)S–C [1.713–1.732(4) Å] and (S=C)S–C [1.745–1.758(4) Å] distances, while in (XI) there is no such difference [1.730–1.751(7) Å and 1.725–1.747(7) Å respectively], which is a probable indication of the greater electron delocalisation in the chelate rings of complex (XI). In the crystals of both (X) and (XI) the $[Au(dmit)_2]^{x-}$ anions form stacks (with some tendency for

dimerisation to occur) along the axes a = 7.425 Å in (X) and b = 7.4186 Å in (XI) [the interplanar distances in the stacks are 3.49 and 3.79 Å in (X) and 3.57 and 3.64 Å in (XI)]. The nature of the overlap of the complexes in the stacks of crystals of (X) and (XI) varies slightly. In the crystal of (X) there is a greater relative longitudinal shift and smaller lateral shift of the anions in comparison with (XI) (Figs. 9 and 10). In (XI) there is only one slightly shortened S(5)...S(8) contact [3.681(2) Å] in the stack in contrast to the three significantly shortened S...S contacts in (X) [S(2)...S(6) at 3.489 Å, S(2)...S(8) at 3.529 Å, and S(6)...S(6) at 3.510(2) Å].

The crystal of (X) is isostructural to the crystal of (IV). As in the crystal of (IV), "dimerisation" of the anions occurs in the stacks of the crystal of (X), the interplanar distances between the planes of $[Au(dmit)_2]^{1/2-}$ anions being 3.49 and 3.79 Å. In the stacks of the crystal of (XI) each Au atom is situated at a distance of 3.620 and 3.849(2) Å from the sulphur atoms of the $[Au(dmit)_2]^-$ anions located in the same stack above and below the reference anion, and the S...Au...S vector is approximately perpendicular to the plane of the reference complex.

While the stacks of $[Au(dmit)_2]^{1/2-}$ anions in the crystal of (X) are combined into layers via a large number of shortened S...S contacts in the [100] direction (3.463–3.525 Å), the presence of twice as many Et_4N^+ cations in (XI) results in an isolated configuration of the stacks of complex anions and the structure of (XI) losing the "two-dimensional" nature that is characteristic of the crystal of (X).

The temperature dependence of the electrical conductivity of crystals of (X) has a semiconductive character. When $(Et_4N)[Au(dmit)_2]$ was oxidised, β-$\{(Et_4N)_{0.5}[Au(dmit)_2]\}$ (the β-form), which has metallic properties, was obtained in addition to the α-form.

There is definite interest in making a detailed comparison of the structures of conductive and nonconductive salts composed of uniform anions and cations but in different ratios, as in the structures of (V) and (IX) or (V) and (XII). This type of comparison is presented below for the structures of (V) and (XII), since the structural information published[46] on salt (IX) is insufficient for a detailed comparison.

On going from the electroconductive stack-layer nonstoichiometric Ni phase of (V) to the Au salt (XII), containing the same cations,

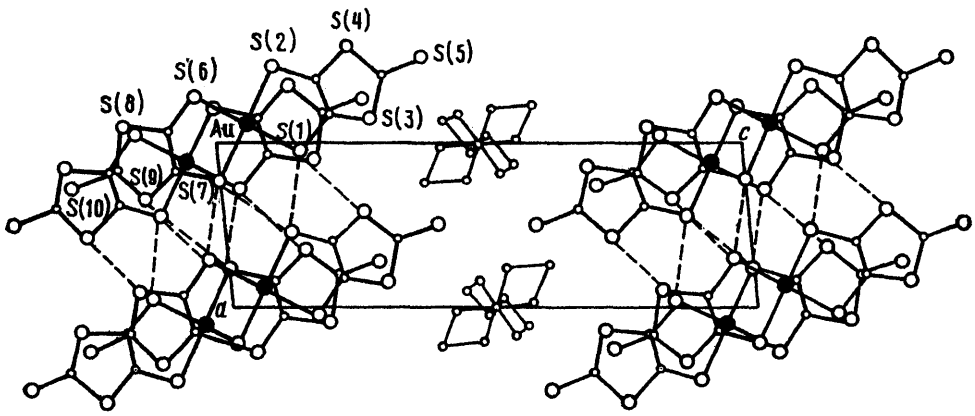


Figure 9. Projection of the crystalline structure of (X) on to the *ac* plane. The Et_4N^+ cations are randomised relative to the centres of symmetry.[47]

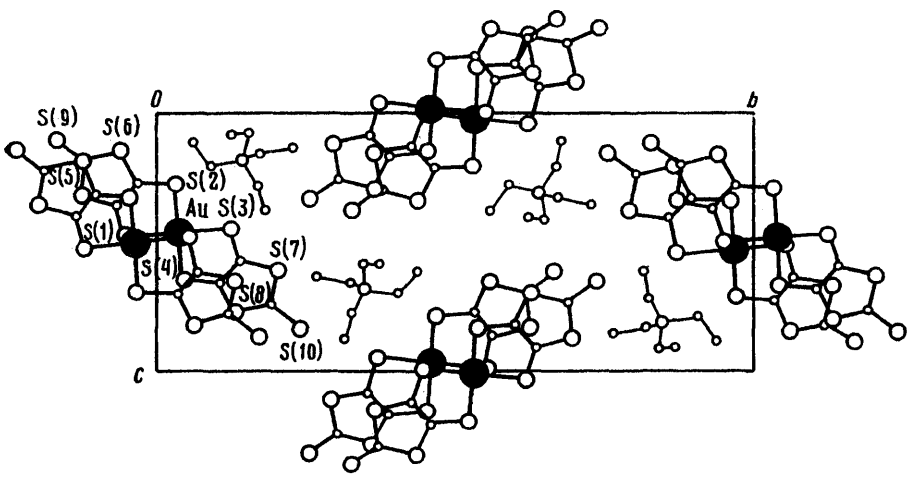


Figure 10. Projection of the crystalline structure of (XI) on to the *bc* plane.[48]

there is a more fundamental structural rearrangement than on going from (X) to (XI). A structure which is only approximately planar (in the two symmetrically independent anions Δ_{max} = 0.11 and 0.19 Å) characterises the $[Au(dmit)_2]^-$ anions of salt (XII). The Au–S distances [2.316–2.327(4) Å] in (XII) are in good agreement with those found in the two Au complexes of the type $Cat^+[Au(dmit)_2]^-$ (see Table 2). In contrast to the structure of (V), there is no conjugation in the (Au)S–C=C–S(Au) chelate residue in the crystal of (XII). The C=C, (Au)S–C, and (S=C)S–C distances in the two symmetrically independent molecules are equal to 1.29 and 1.30(2) Å, 1.73–1.76(1) Å, and 1.75–1.76(1) Å respectively.

In the crystal of (XII) the $[Au(dmit)_2]^-$ anions do not form stacks, and the symmetrically independent anions A and B which alternate along the *a* axis are not parallel, the dihedral angle between their planes being 76.2° (Fig. 11). There is only one shortened S(2)...S(8′) contact [3.565(5) Å] between the A and B anions. Between the B anions, related by (½, ½, ½) centres of symmetry, there are several shortened S(8′)...S(8″) contacts [3.495(5) Å], which form infinite chains of anions along the [011] direction. A parallel arrangement of anions A and B, in other words, the formation of stacks in the crystal of (XII), is prevented by the Bu_4N^+ cations, which are "wedged" between the anions, forming layers together with the anions parallel to the (010) plane.

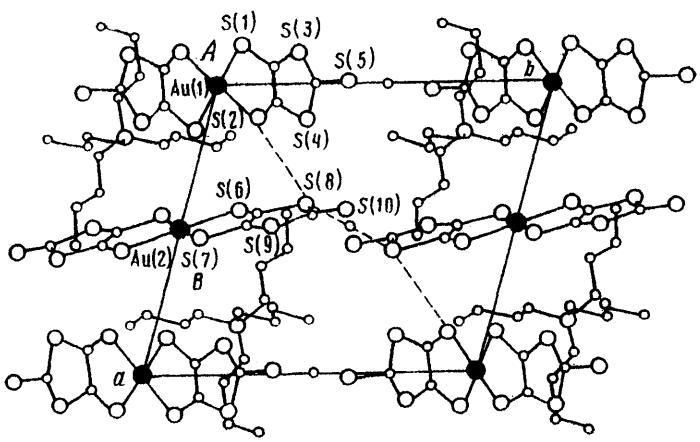


Figure 11. Projection of the crystalline structure of (XII) on to the *ab* plane.[49]

The salt $(Me_3S)[Au(dmit)_2]$ (XIII) has a structure which is quite distinct from other salts of the type $Cat_x^+[M(dmit)_2]^{x-}$ listed in Table 2. In fact, in the crystal of (XIII), which, like the crystal of (XII), is composed of two symmetrically independent anions A(1) and A(2) and cations Cat(1) and Cat(2), all anions are essentially parallel to each other (the dihedral angle between the planes of A(1) and A(2) is 1.0°) and to within about 0.1 Å occur in the same plane $(21\bar{3})$ passing through the centres of symmetry (0, ½, 0), (1, 0, ½), and (½, 1, ½) (Fig. 12). The neighbouring anion planes are separated from this plane by a distance of 3.59 Å, related to each other by the translation *a* or by centres of symmetry of the type (½, ½, ½). The Me_3S^+ cations on the edges of the layer form rows along the $[2\bar{1}1]$ direction.

At the edges of a layer in the structure of (XIII) it is possible to distinguish three types of interanion S...S contact responsible for electrical conductivity. A considerably shortened S(10)...S(10′) distance [3.128(4) Å] occurs between the A(1) anions related by a (½, 1, ½) centre of symmetry. This is the shortest intermolecular S...S distance of those found for potentially electroconductive S-containing compounds. A similar but slightly greater S...S distance (3.16 Å) occurs between stacks of planar anions in the crystal of $Li_{0.75}[Pt(C_4N_2S_2^{2-})_2].2H_2O$ ($H_2C_4N_2S_2$ is 1,2-dicyanovinylene-1,2-dithiol, σ_{293} = 30–212 Ω^{-1} cm^{-1}).[59]

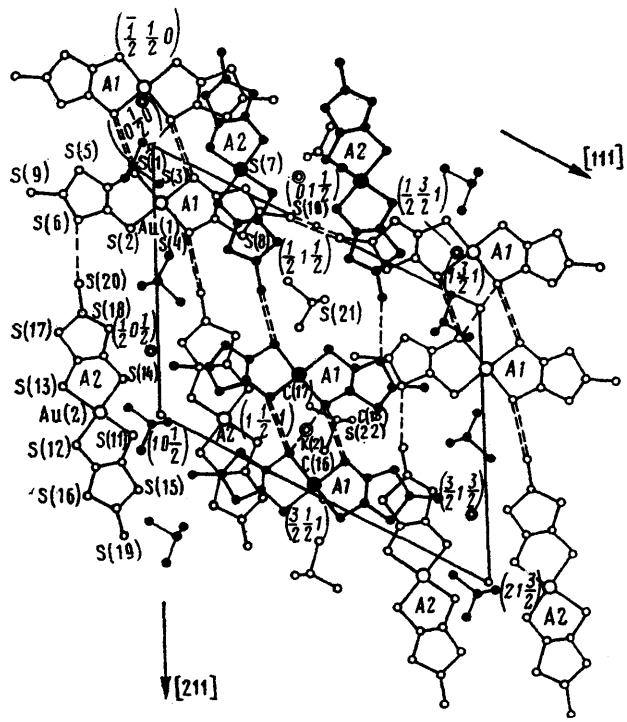


Figure 12. Projection of the crystalline structure of (XIII) on to the plane of the $[21\bar{3}]$ layer. Two layers (light and dark circles) are shown.[50]

The second group comprises shortened contacts [3.407(4) Å] between S(4)...S(19) atoms related by a (1–*x*, –*y*, 1–*z*) centre of symmetry) and S(1)...S(3) atoms [3.478(4) Å] related by a (–*x*, 1–*y*, –*z*) centre of symmetry. These contacts are appreciably less than twice the van der Waals radius of the S atom. Finally, the third group comprises contacts that are slightly less or approximately equal to twice the van der Waals radius of the S atom: S(1)...S(1), (–*x*, 1–*y*, –*z*), 3.572(4) Å; S(6)...S(20), (1 + *x*, *y*, *z*) 3.588(4) Å; and S(3)...S(5), (–*x*, 1–*y*, –*z*) 3.679(4) Å.

The layers are superimposed in such a manner that the rows of cations of each layer extending along the [211] direction occur between the rows of anions of the neighbouring layers and *vice versa* (anions between cations, Fig. 12). The shortest S...S distances between layers are nearly equal to twice the van der Waals radius of the S atom and are contacts of the type anion...cation: S(1)...S(21), (*x*, *y*, *z*), 3.654(4) Å and S(11)...S(22), (–*x*, –*y*, 1–*z*), 3.688(4) Å.

Table 3. The main data on $D[M(dmit)_2]_x$ compounds (D = donor molecule).

Compound	Chemical formula	Structural motif	M–S distance, Å	Conductivity** σ_{293}, Ω^{-1} cm^{-1}	Refs.
(XV)	$(TTF)[Ni(dmit)_2]_2$	Segregated stacks of D (d=3.65 Å) and A (d=3.55 Å)→mixed layers →quasi-three-dimensional structure	2.161–2.172 (8)	300 (metal)	[57, 58]
(XVI)	$(TSF)[Ni(dmit)_2]_3$	Stacks of A (d=3.54 and 3.63 Å)→layers of A	2.152–2.165	4 (semiconductor)	[61]
(XVII)	$(TMTSF)[Ni(dmit)_2]$	Segregated stacks of D (d=3.75 Å) and A	see*	300 (semiconductor)	[62]
(XVIII)	$(DBTTF)[Ni(dmit)_2]$	Segregated stacks of D (d=3.53 Å) and A (d=3.55 Å)	see*	300 (metal)	[63]
(XIX)	$(BEDT–TTF)[Ni(dmit)_2]$	Mixed stacks of D and A. Shortened contacts between stacks	see*	0.02 (semiconductor)	[64]
(XX)	α-$\{(BPDT–TTF)[Ni(dmit)_2]_2\}$	Segregated stacks of D and A; dimerisation of stacks of A	see*	10 (semiconductor)	[65]
(XXI)	$(TTF)[Pt(dmit)_2]_3$	Stacks of A consisting of alternating monomers and dimers→layers of A	2.29–2.32 (1)	20 (semiconductor)	[58]
(XXII)	$(HMTTeF)[Pt(dmit)_2]_{0.5}$	Tetrads of D (d=3.62 and 3.70 Å)→layers of D	see*	20 (semiconductor)	[66]

*Not in the original study.
**If the values of σ in the different crystallographic directions differ, the maximum values are given here.

The crystal of (XIII) is an insulator ($\sigma_{293} \approx 10^{-5}$ Ω^{-1} cm^{-1}). Oxidation of compound (XIII) with iodine gives a product with good conductivity ($\sigma_{293} \approx 30$ Ω^{-1} cm^{-1}), whose composition and structure have so far not been established.[50]

III. Structure of salts of 4,5-dimercapto-2-thione-1,3-dithiolates with "open" cations

A basic feature of the compounds examined in this section is the participation of both donor molecules and acceptor molecules in the formation of electroconductive corridors. We should also point out the difference between salts of "open" cations† and organic conductors of the type TTF–TCNQ[1–3] or $(TTF)[Ni(mnt)_2]$[60] (mnt = maleonitrilo-1,2-dithiolate), for example, in which the electroconductivity can in principle be related to the presence of donor stacks (in the first case) or acceptor stacks (in the second). In fact, in layers of $Cat_x^+[M(dmit)_2]^{x-}$ of the type TTF or BEDT–TTF (Table 3) both the cations of the donor and the anions of the acceptor contain a large number of sulphur atoms, which helps to increase the dimensionality of electroconductive motifs.

Crystals of $(TTF)[Ni(dmit)_2]_2$ (XV) are composed of segregated stacks of donors and acceptors extended along the [010] direction. The molecule of the donor (TTF) is completely planar while the molecule of the acceptor $Ni(dmit)_2$ is slightly bent (by 4.4°). The translation along the b axis is equal to 3.73 Å, but because both molecules—TTF and $Ni(dmit)_2$—are inclined towards the (010) plane, the intrastack interplanar distances d are less (in the donor stacks the molecules are inclined towards the (010) plane by 12° and d = 3.65 Å and in the acceptor stacks the molecules are inclined by 18° and d = 3.55 Å).

The intrastack S...S distances in the donor stacks are slightly less than in the acceptor stacks. Moreover, there are a large number of shortened intermolecular interstack S...S contacts involving molecules of both donor and acceptor in the crystal of (XV) (Fig. 13). Thus, between the $Ni(dmit)_2$ molecules of neighbouring stacks in the [001] direction there are S...S contacts (3.45 Å) which lead to the formation of a two-dimensional layer motifs of closely packed molecules of donor and acceptor located in the (100) plane. The even closer S...S contacts (3.38 Å) between the terminal S atoms of the $Ni(dmit)_2$ molecules and the TTF molecules convert the whole system of donor and acceptor molecules interacting in the crystal of (XV) into a three-dimensional arrangement. The high dimensionality of the structure assists the transition of the crystal of (XV) to a superconductive state at 1.62 K and 7 kbar.[58]

In contrast to TTF, its selenium analogue (TSF) forms a semiconductive phase of composition 1:3—$(TSF)[Ni(dmit)_2]_3$ (XVI)—with the $Ni(dmit)_2$ complex. The crystal of (XVI) is composed of two symmetrically independent $Ni(dmit)_2$ molecules (A at the centre of symmetry, B at a general position) and a TSF molecule (at the centre of symmetry). The length of the central C=C double bond in the TSF molecule is increased to 1.431 Å; this suggests that there is significant delocalisation of π-electron density in the donor molecule, which is typical for its cationic state $(TSF)^+$.[67] The lengths of the Ni–S bonds in molecules of A (2.153 and 2.165 Å) and B (2.152–2.163 Å) do not differ. In both types of anion, delocalisation of electrons occurs in the (Ni)S⩶C⩶C⩶S(Ni) residues; the C=C bond lengths are equal to 1.380 Å (A) and 1.380 and 1.393 Å (B), and the (Ni)S–C

†Cations of an "open" donor participate in electron transfer.

distances of 1.689 and 1.702 Å (A) and 1.688–1.708 Å (B) are appreciably less than the (S=C)S–C distances of 1.744 and 1.745 Å (A) and 1.739–1.743 Å (B).

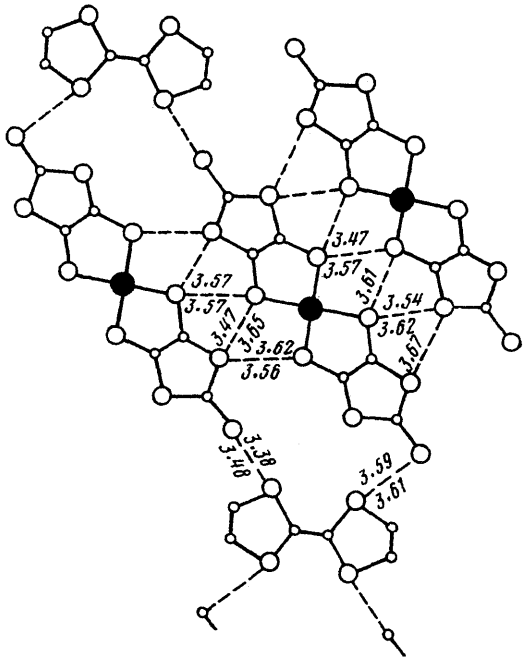


Figure 13. Part of the crystalline structure of (TTF)[Ni(dmit)$_2$]$_2$ (XV) (projection on to the *ac* plane).[57,58]

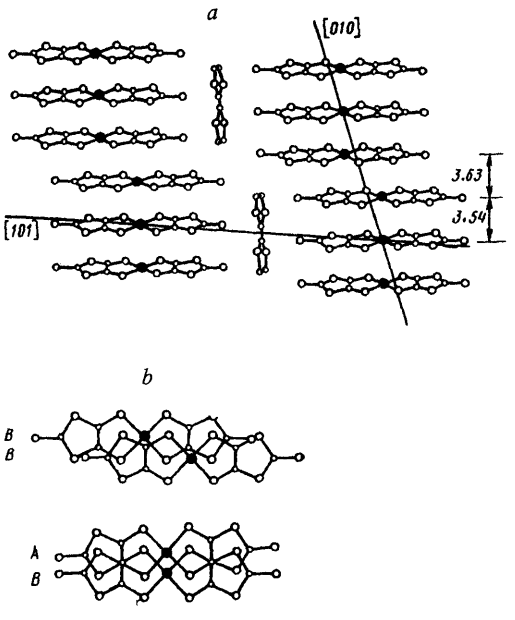


Figure 14. Crystalline structure of (TSF)[Ni(dmit)$_2$]$_3$ (XVI): *a*) relative configuration of the molecules of donor (TSF) and acceptor Ni(dmit)$_2$ (the interplanar distances in the centrosymmetric triads formed in the acceptor stacks are given); *b*) the two types of overlap of Ni(dmit)$_2$ molecules—A...B (within triads) and B...B (between triads).[61]

The Ni(dmit)$_2$ acceptor molecules are located parallel to each other with a slight shift and form BAB triads stacked along the *b* axis, with the interplanar distances within the triads equal to 3.54 Å (3.63 Å between the triads) (Fig. 14). The normal to the plane of the Ni(dmit)$_2$ complex forms an angle of 26° with the *b* axis of the crystal of (XVI). The stacks of acceptor molecules form via S...S contacts (3.503–3.646 Å) layers that are perpendicular to the [101] direction, between which are located TSF molecules not forming stacks. There are a number of shortened S...Se contacts (3.417–3.587 Å) between the terminal S atoms of the Ni(dmit)$_2$ complexes and Se atoms of the TSF molecules (sum of the van der Waals radii of S and Se atoms is 3.85 Å).[51]

When the temperature is lowered to 65 K in crystals of (XVI) a phase transition occurs, which is accompanied by a doubling of the spacing *a* and which appears to have a one-dimensional character of spin-Peierls type.[61] The shortest S...S distances occur along the *a* axis in the crystal of (XVI)—the anion stacks interact to form layers. Thus, this phase transition is probably related to dimerisation in the layers of acceptor molecules. It has been noted[61] that the spins of Ni(dmit)$_2$ complexes make a very small contribution to the total magnetic moment of the crystal of (XVI) and the total magnetic susceptibility of (XVI) is determined by TSF molecules, which have an unpaired electron that behaves as a virtually free spin, being related to the almost perpendicular relative configuration of Ni(dmit)$_2$ and TSF molecules and the large distance between TSF molecules [there are no short Se...Se contacts in the crystal of (XVI)]. On lowering the temperature (below 65 K) the spins of the TSF molecules start to line up.

A model has been proposed[56] to account for the magnetic behaviour of (XVI)—at temperatures >150 K the magnetic moment is independent of temperature and constitutes 2.1 B.M. On lowering the temperature to ~100 K the magnetic moment starts to decrease. The curve of magnetic susceptibility (χ) reaches a maximum at ~20 K, below this temperature χ decreases rapidly.

The conductive properties of crystals of (XVI) are mainly determined by the two-dimensional system of Ni(dmit)$_2$ molecules. The resistance of crystals of (XVI) along the *a* axis is very small (0.25 Ω cm) and increases monotonically on lowering the temperature.

A previous X-ray diffraction study of (TMTSF)[Ni(dmit)$_2$] (XVII) showed that the lattice of (XVII) is modulated sinusoidally. With a spacing of 9*b* on the X-ray photograph, there are satellite reflections which indicate that a ninefold superlattice occurs. The parameters of the unit cell of the superlattice are: a=15.227(4) Å, b=34.559(5) Å, c = 25.455(6) Å, β = 105.70(2)°, V = 12895(5) Å^3, Z = 18, space group $P2_1/n$. The vectors of the units cell of the fundamental lattice are given by $\mathbf{a}_0 = \mathbf{a}$, $\mathbf{b}_0 = \mathbf{b}/9$, $\mathbf{c}_0 = \mathbf{c}$. The wave amplitude of the periodic distortion of the lattice (PDL) was determined from the variation in intensities of the main and satellite reflections.

The fundamental structure of (XVII) is shown in Fig. 15. Molecules of TMTSF and Ni(dmit)$_2$ forms segregated stacks along the axis $b_0 = b/9 = 3.840$ Å. In the stacks the molecules of TMTSF donor are almost completely superimposed on each other, the interplanar distance *d* being equal to 3.75 Å. On the other hand, in the stacks of acceptor molecules overlap is small. The TMTSF and Ni(dmit)$_2$ molecules form a dihedral angle of 27°.

An important role in determining the direction of electron transfer is played by the anisotropy of the intermolecular overlap integrals (S) of the HOMOs of donor molecules and/or LUMOs of acceptor molecules. The transfer integral (t) is approximately proportional to S ($t \approx -ES$, where E is a constant). In accordance with the close

contacts and precise overlap of the molecules in the stacks of TMTSF, the width of the corresponding energy zone in (XVII) is twice as great as in stacks of salts of the type $(TMTSF)_2X$.[68] In the $Ni(dmit)_2$ stacks the overlap integral is very small. It has been noted[57] that the Fermi surface of the crystal of (XVII) has a flattened profile and is perpendicular to the *b* axis (the direction of the stacks). In contrast to the holes in the TMTSF stacks, the electrons in the $Ni(dmit)_2$ stacks have low mobility, which may be related to the small values of the overlap integrals along the stacks.

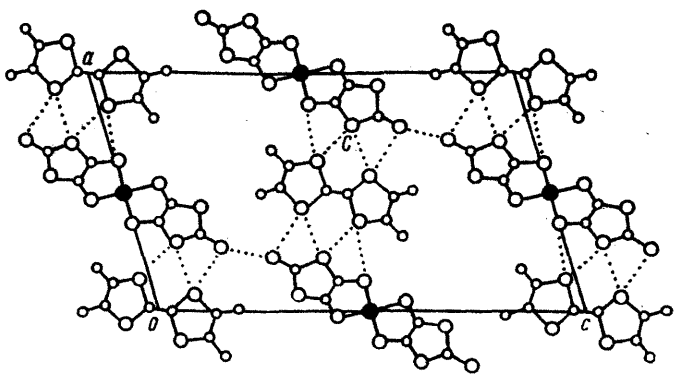


Figure 15. Projection of the main structure of (XVII) along the $\bar{b}_0$ direction. Interstack S...S contacts are shown as dotted lines.[62]

It has been noted by Kobayashi et al.[62] that when there is a planar form of the Fermi surface, if the structure is not modulated the system must be a one-dimensional metal. The observed semiconductive nature of the crystal of (XVII) is evidently due to the occurrence of PDL. It is known that a Peierls distortion with a period of $2k_F$ or PDL with a frequency of $2k_0$ can destabilise the metallic state. The existing experimental data suggest that in this case the semiconductive nature of (XVII) is due to the existence of PDL with a period of $2k_0$. Thus, in contrast to single-chain systems in which the main mechanism for disruption of stability is a Peierls distortion, destabilisation in double-chain systems with intersecting energy zones [an example of which is the crystal of (XVII)] may be caused by transverse PDL waves. The relatively large interchain interaction and large amplitude of the PDL wave are responsible for the behaviour of crystals of (XVII) as a narrow-zone semiconductor.

The structure of (XVIII) is similar to the structure of (XVII); DBTTF and $Ni(dmit)_2$ molecules form segregated stacks directed along the short axis *b* = 3.830(5) Å. The normals to the planes of the donor and acceptor molecules deviate in different directions from the line of the *b* axis and form angles of 23° and 22° respectively with it, namely, the cation planes are not parallel to the anion planes and intersect them at an angle of 135° (Fig. 16). The superimposition of molecules in both types of stacks occurs with a small (~1–1.5 Å) relative shift of the molecules in directions perpendicular to their long axes. In contrast to the structure of (XVII), the interplanar distances in the donor and acceptor stacks in the structure of (XVIII) are similar (3.53 and 3.55 Å), and there are no shortened intermolecular distances in the stacks of either type. Shortened contacts occur between DBTTF and $Ni(dmit)_2$ molecules that belong to neighbouring stacks along the *a* axis, which leads to a two-dimensional type of structure for (XVIII) (layers parallel to the *ab* plane). The *B*1 and *B*2 overlap integrals in the stacks (and, hence, the width of the forbidden zone) are comparable to those calculated for the system TTF–TCNQ.[69] However, in (XVIII) the ratio σ_b (within stacks): σ_a (between stacks) ≈10, i.e., less than in TTF–TCNQ, where it is ~10^2 and close to that found in $(TMTSF)_2X$ salts.[68] The overlap integrals along the *c* axis of the crystal of (XVIII) also have an appreciable value, which can suggest that there is also a significant electronic interaction in a third direction (perpendicular to the layers). For a double-chain donor-acceptor system when the interaction between frontier orbitals from different stacks is neglected, zone structures of two types are possible: with two intersecting mutually inverted dispersion curves and with "parallel" overlapping but not intersecting dispersion curves.[63] In the first case the overlap integral between the corresponding frontier orbitals of molecules in one of the stacks (S_1) has a sign opposite to that of the corresponding overlap integral (S_2) in the other stack. In the second case the signs of S_1 and S_2 are the same. Examples of systems of the first type are TTF–TCNQ[69] or (TMTSF)[Ni(dmit)$_2$] (XVII).[62] In these systems the position of the

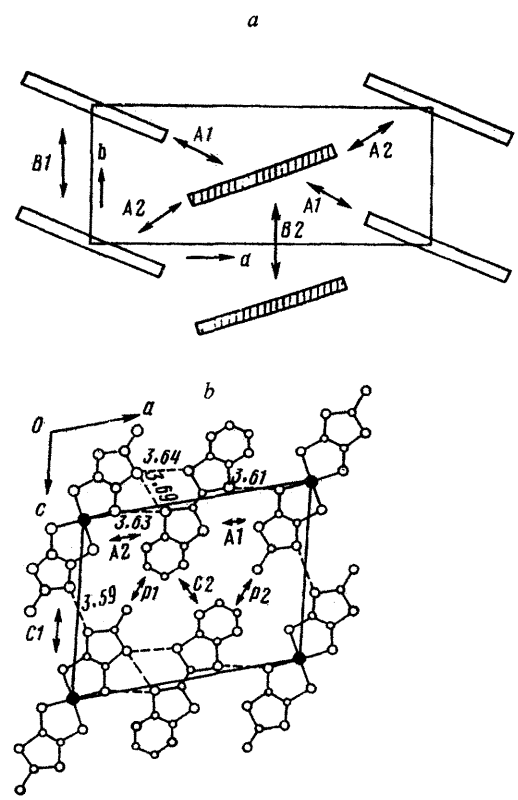


Figure 16. Crystalline structure of (DBTTF)[Ni(dmit)$_2$] (XVIII). *a*) Relative inclination of donor molecules and acceptor molecules (hatched); *b*) shortened intermolecular S...S contacts combining the donor and acceptor molecules into layers parallel to the *ab* plane. The main types of paired intermolecular interactions for which the overlap integrals of the HOMOs of the donor and LUMOs of the acceptor have been calculated are shown ($\times 10^3$): *B*1–12.72 (donor stack), *B*2–9.46 (acceptor stack), *A*1 0.875, *A*2 0.731, *C*1–0.208, *C*2 0.358, *P*1–0.307, and *P*2–0.119 (between stacks).[63]

Fermi level corresponds to the point of intersection of the dispersion curves. When the (donor–acceptor) stacks interact, the metallic state becomes unstable. The energy level that corresponds to the Fermi energy is split and a zone structure characteristic of semiconductors with a zero width of the forbidden zone is possible.[70]

In the case of the crystal of (XVIII) the overlap integrals S_1 and S_2 for the stacks of DBTTF and Ni(dmit)$_2$ respectively have the same sign. In this case the dispersion curves are "parallel". Therefore the metallic state proves stable in relation to interstack interaction. This phenomenon is responsible for the special interest in the low-temperature electrical properties of (XVIII). According to initial measurements, the electrical conductivity of (XVIII) is very high (σ_{293}, $b \approx 300\ \Omega^{-1}\ cm^{-1}$), and on lowering the temperature the value of σ_b shows very little change.

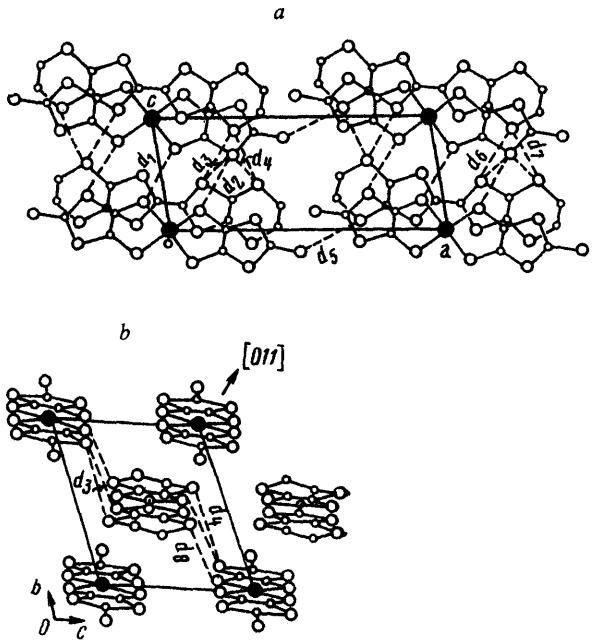


Figure 17. Crystalline structure of (BEDT–TTF)[Ni(dmit)$_2$] (XIX): *a*) projection on to the *ac* plane parallel to the plane of Ni(dmit)$_2$; *b*) projection on to the *bc* plane. The [011] direction of mixed stacks of donor and acceptor is shown. Broken lines represent the shortened interstack S...S contacts with distances d_1 = 3.53, d_2 = 3.65, d_3 = 3.65, d_4 = 3.63, d_5 = 3.58, d_6 = 3.52, d_7 = 3.41, d_8 = 3.68 Å.[64]

In contrast to the salts (XV)–(XVIII) examined above, whose structures are composed of segregated donor and acceptor stacks, in the crystal of (BEDT–TTF)[Ni(dmit)$_2$] (XIX) there are mixed stacks along the [011] direction (Fig. 17). Despite the clear overlap of cations and anions in the stacks, there are no shortened S...S contacts within the stacks probably because of the presence of the terminal ethylene spacers in the BEDT–TTF molecules. At the same time, there are quite a number of shortened S...S contacts along the [001] direction, in other words, there is a tendency which is characteristic of BEDT–TTF and M(dmit)$_2$ molecules to undergo "face" interactions.

The electrical conductivity of the crystal of (XIX) in the [001] direction at 300 K is $\sigma^{\parallel}_{300} = 0.02\ \Omega^{-1}\ cm^{-1}$ (the ratio $\sigma^{\parallel}/\sigma^{\perp} \approx 0.66$); on lowering the temperature the conductivity decreases. The energies of activation of electrical conductivity $\sigma^{\parallel}$ and $\sigma^{\perp}$ are almost equal (0.28 eV). As was noted by Kobayashi et al.,[64] all of the previously studied charge-transfer complexes (CTC) with mixed stacks were insulators, therefore the relatively high conductivity of the crystal of (XIX) caused considerable interest. Kobayashi et al.[62] have made a detailed review of physical models used to account for this phenomenon.

For a linear chain (stack) of alternating donor (D) and acceptor (A) molecules extending along the *c* axis (Fig. 18*a*) with a simple approximation of a strong bond, one-dimensional energy zones are formed by the frontier orbitals (HOMOs of the donor and LUMOs of the acceptor). It can be shown that the energy gap of such a system ($E_A - E_D$) (E_A and E_D are the energies of the LUMOs and HOMOs) is not decreased by an intermolecular interaction, and CTCs with mixed stacks are insulators. If the interaction between stacks is significantly greater than along them, molecules of D and A form segregated zones in a lateral direction (Fig. 18*b*).

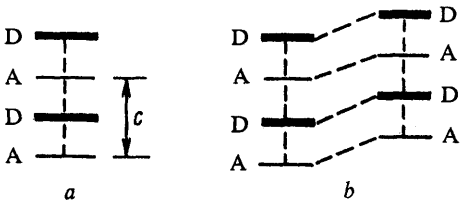


Figure 18. Two ways of arranging the molecules of donor (D) and acceptor (A) in the crystal of a CTC with mixed stacks. The direction of the main interaction between molecules of D and A is shown as a broken line.[64]

Taking into account the anisotropy of the π-orbitals, it could be assumed that the lateral intermolecular interactions in organic conductors must be small. However, calculations of the zone structure show that for molecules of the type BEDT–TTF, lateral (and/or tangential) interactions may be considerable. Calculation of the overlap integrals (*S*) of the frontier orbitals of BEDT–TTF (D) and Ni(dmit)$_2$ (A) in the crystal of (XIX) using the EH method gave the following values:[64] for contact D(x, y, z)...D(x, y, z + 1) the value of $S \times 10^3$ is 2.26, for D(x, y, z)...A(x, y, z + 1) it is 1.14, for D(x, y, z)...A(x, y, z) it is 0.75, for A(x, y, z)...A(x, y, z + 1) it is 0.28, and for D(x, y, z)...A(x + 1, y + 1, z) it is 0.11. It was noted by Kobayashi et al.[64] that since the symmetry of the HOMOs (BEDT–TTF) and LUMOs [Ni(dmit)$_2$] are different, the overlap integrals of D...A along the [011] direction in the crystal of (XIX) can be neglected. The integral of lateral overlap D(x, y, z)...D(x, y, z + 1) has the highest value, in other words, it is possible to consider segregated motifs formed by BEDT–TTF in a lateral direction relative to the stacks in the crystal of (XIX) (see also the study of Mori et al.).[71]

Kobayashi et al.[64] regard salt (XIX), which is characterised by partial D→A charge transfer and a fairly strong lateral interaction between BEDT–TTF molecules, as a novel type of organic metal, although the overlap integral (*S*) of the frontier orbitals of

BEDT–TTF molecules in (XIX) is not very large. It is known that the overlap integral of BEDT–TTF molecules is determined by the "configurational" parameters R and φ, which are governed by the relative‡ orientation of neighbouring molecules.[71] The relative orientation of BEDT–TTF molecules in the crystal of (XIX) is such that the value of S proves to be 5–10 times less than in the superconductor β-(BEDT–TTF)$_2$I$_3$.[72]

The crystal of the salt α-{(BPDT–TTF)[Ni(dmit)$_2$]$_2$} (XX), which differs from the crystal of (XIX) in its ratio of donor to acceptor and the even less planar structure of the donor molecule [because of the presence of an additional methylene group in the side rings of the molecule of (XX)], is composed of segregated stacks of donor and acceptor molecules, the acceptor stacks forming paired chains.[65] At room temperature (300 K) the electrical conductivity of (XX) is 5–10 Ω^{-1} cm^{-1} and progressively decreases as the temperature is lowered to 120 K. Below 120 K (XX) undergoes a transition to a nonconductive state. An X-ray diffraction study was carried out on salt (XX) at 293 and 96 K and no substantial differences in the structure of crystals of (XX) were detected at the different temperatures. Nevertheless, the overlap integrals of the frontier molecular orbitals, calculated for salt (XX) at 293 and 96 K, are somewhat different, which suggests that there is a strengthening of the lateral S...S interaction between the paired stacks of Ni(dmit)$_2$ in the crystal recorded at 96 K. Kobayashi et al.[65] have proposed a mechanism for the transition of (XX) to a nonconductive state, requiring only a small change in the degree of charge transfer and hence not producing significant changes in the crystalline structure of (XX) on going from 293 to 96 K.

The salt (TTF)[Pt(dmit)$_2$]$_3$ (XXI) has the same ratio of donor to acceptor as salt (XVI) (1 : 3 in both cases) and has similar parameters of its unit cell. However, it has an unusual feature which does not occur in any of the M(dmit)$_2$ salts; one of the crystallographically independent complexes Pt(dmit)$_2$ complexes forms a centrosymmetric dimer via a direct Pt–Pt bond of length 2.935 Å. Despite the formation of the Pt–Pt bond, the increase in basal Pt–S distances in the [Pt(dmit)$_2$]$_2$ dimers is small. In the dimer the Pt–S bond lengths are 2.30–2.32(1) Å, and in the monomer they are 2.29–2.30(1) Å. In the sterically less strained neutral dimer [Pt(S$_2$C$_2$H$_2$)$_2$]$_2$ the Pt–Pt distance is somewhat less (2.748 Å).[73] As in the [Pt(S$_2$C$_2$H$_2$)$_2$]$_2$ complex, the planarity of both parts of the dimer in [Pt(dmit)$_2$]$_2$ is considerably distorted, the dihedral angle between the two Pt(dmit) residues in each half of the dimer being 11.2°. The second crystallographically independent Pt(dmit)$_2$ anion remains in the crystal of (XXI) in monomer form and occupies a particular position at the centre of symmetry like the TTF molecule.

The structural motif of the crystal of (XXI) resembles that of (XVI)—layers of monomers and Pt(dmit)$_2$ dimers are parallel to the (001) plane and alternate with layers of TTF molecules. In the acceptor layers, stacks are distinguishable along the [1$\bar{1}$0] direction in which monomers and dimers alternate. The normal to the average plane of the Pt(dmit)$_2$ monomer and also the Pt–Pt bond in the dimer form similar angles (~23°) with the [1$\bar{1}$0] direction (stack axis).

‡For two molecules of BEDT–TTF which are parallel but displaced, the value of R is the relative displacement of the molecules along their long axes, and φ is the angle between the vector joining the long axes of the molecules (and that perpendicular to them) and the plane of the molecule (see, for example, Mori et al).[71]

In contrast to the crystal of (XVI), in which shortened intermolecular distances (of the type S...Se) occur only between molecules of acceptor (superimposed in stacks) and donor (located between stacks), in the crystal of (XXI) there are a considerable number of shortened S...S contacts: in the stacks within the dimers (four contacts of length 3.23–3.66 Å, inducing intramolecular contacts), in the stacks between the monomers and dimers (four contacts of length 3.63–3.66 Å), and between the Pt(dmit)$_2$ residues of monomers or dimers of neighbouring stacks (17 contacts of length 3.47–3.65 Å). On the whole the shortened S...S contacts between the acceptor molecules result in the formation in the crystal of (XXI) of the above-mentioned acceptor layers, parallel to the (001) plane. The donor molecules only participate in a single shortened intermolecular contact with the Pt(dmit)$_2$ monomer (a distance of 3.45 Å) and there are no shortened contacts of the type TTF...TTF in the crystal of (XXI).

The crystal of (XXI) is a semiconductor in the temperature range 300–100 K. The observed thermally activated electrical conductivity is probably due to the alternation of monomer and dimer molecules in the Pt(dmit)$_2$ stacks, resulting in the formation of a gap in the zone structure in the region of the Fermi level. Nevertheless, the electrical conductivity of the crystal of (XXI) at room temperature is unexpectedly high (20 Ω^{-1} cm^{-1}), which Bousseau et al.[58] thought could be due to significant interstack interaction.

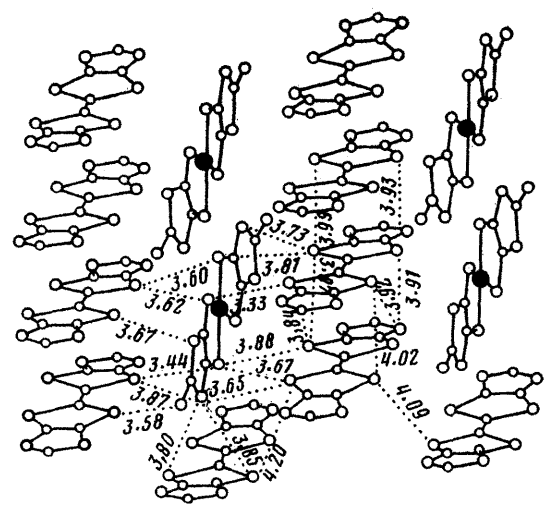


Figure 19. Short intermolecular contacts involving chalcogenide atoms in the crystal of (HMTTeF)[Pt(dmit)$_2$]$_{0.5}$ (XXII).[66]

For the crystal of (HMTTeF)[Pt(dmit)$_2$]$_{0.5}$ (XXII), the electrical conductivity at room temperature (20 Ω^{-1} cm^{-1}) and semiconductive nature of the temperature dependence of conductivity are found to be the same as for (XXI). The HMTTeF molecules are packed in the crystal of (XXII) (Fig. 19) into centrosymmetric stacks (tetrads), each with four molecules (two of them are crystallographically independent).

The interplanar distances in the tetrads are 3.62 and 3.70 Å. One of the crystallographically independent HMTTeF molecules is planar, the second is slightly bent along the line of Te...Te of one of

the heterocycles (by 9°). The tetrad stacks are combined into a two-dimensional system through short Te...Te contacts. The $Pt(dmit)_2$ complexes are located between the tetrad systems of HMTTeF molecules, the planes of the anions being approximately perpendicular to the planes of the HMTTeF molecules.

In the crystal of $(HMTTeF)_4(PF_6)_2$, the first CTC based on HMTTeF to be studied using X-ray diffraction, the HMTTeF molecules are arranged in stacks possessing a triad structure; the fourth (neutral) HMTTeF molecule is located between the stacks, with its plane parallel to the stack axis.[74] A similar structural motif also occurs in the monoclinic phase of β-$(HMTTeF)_2(PF_6)$.[66] It was noted by Kato et al.[75] that this type of packing is typical for salts with well-defined two-dimensional motifs.

The overlap integrals (S) of the HOMOs of HMTTeF molecules in the tetrads of (XXII) (-65.58×10^{-3} and 60.28×10^{-3}) are considerably higher than in other chalcogenfulvalene derivatives (for example, $S = 5\times10^{-3}$ in the TTF stacks of the salt TTF.TCNQ[69] and $S = 40\times10^{-3}$ in the TMTSF stacks of the salt (TMTSF)[Ni(dmit)$_2$] (XVII)[62]). The overlap integrals of the frontier orbitals of HMTTeF molecules of nieghbouring tetrads constitute about one third of the corresponding overlap integrals within the tetrads. The zone structure of (XXII) was calculated with a simple approximation of a strong bond.

It is difficult to determine experimentally the degree of charge transfer in salt (XXII) (from bond lengths, for example) because of the absence of accurate structural data on salts of the donor HMTTeF occurring in difference valence states.[66] If the formal charge x of the $[Pt(dmit)_2]^x$ complex is assumed to be equal to -1.0, as in the initial salt $(Bu_4N)[Pt(dmit)_2]$, the energy zone of (XXII) is 3/4 full. It follows from a calculation of the zone structure that compound (XXII) is not a metal. It is interesting that the hypothetical compound with the same composition as (XXII) but with a diad stack structure is characterised by the same form of Fermi surface as that calculated for the superconductor β-$(BEDT-TTF)_2I_3$,[76] but with a considerably wider conductivity zone than in known molecular metals,[66] which is an indication of the potentiality of the donor HMTTeF in the molecular design of low-dimensional metals.

Molecular donor-acceptor π-complexes of the type (TTF)[M(dmit)$_2$]$_x$ have all the required properties for high electrical conductivity: planarity of the donor and acceptor components, sufficiently compact and segregated stacks, substantial systems of conjugation and effective intermolecular π-overlap, and similar values of the redox potentials of donor and acceptor. Complexes of the type (TTF)[M(dmit)$_2$]$_x$ have a tendency to form two-dimensional systems, which removes the problem of Peierls distortions in one-dimensional metallic systems. This is shown particularly clearly for the compound (TTF)[Ni(dmit)$_2$]$_2$ (XV), whose high conductivity is retained down to 4 K, and at 1.6 K it undergoes a transition to a superconductive state.[76] It has been noted[56] that such behaviour of (TTF)[Pt(dmit)$_2$]$_2$ is unique for molecular donor-acceptor π-complexes that have a maximum electrical conductivity at temperatures well above 4 K (see, for example, two studies[77,78]) and is due to the presence of an extended three-dimensional network of shortened intermolecular S...S contacts in the crystal of (XV).

It was mentioned above that a distinctive feature of molecular π-complexes of the type D[M(dmit)$_2$]$_x$ (as opposed to Cat$_x$[M(dmit)$_2$] salts) is the possibility of both donor and acceptor molecules participating in the formation of electroconductive channels. In principle, by varying the molecules of donor and acceptor in the two-stack system (in which each type of stack forms its own electroconductive channel), and hence by varying the type of interaction between the stacks in layers, it is possible to obtain conductors with different properties. However, in some cases the strong interstack interaction may lead to the formation of an energy gap. In order to identify the causes of this effect, which is unfavourable for conductivity, a quantum-chemical calculation of the molecules of donor and acceptor, a study of the way in which stacks are formed and combined, and a study of the effect of the cation/anion ratio on the structure of the molecular complex are required.

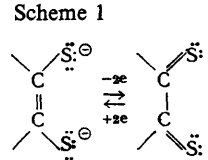
Finally, we should mention once again that D[M(dmit)$_2$]$_x$ salts (D is an open donor) have the highest conductivity among molecular solids in general and among transition metal complexes in particular. Thus, for example, the electrical conductivity of needle-shaped monocrystals of (XV) along the [010] direction (needle axis is direction of segregated stacks of donor and acceptor) is $\sigma_{293} = 300\ \Omega^{-1}\ cm^{-1}$; over the range 300–4 K the temperature dependence of electrical conductivity is of a type characteristic of metals.

IV. Crystalline structures of 5,6-dihydro-1,4-dithiin-2,3-dithiolate complexes and their salts

There is clearly a close similarity between the molecular structure of 5,6-dihydro-1,4-dithiin-2,3-dithiolates of transition metals Cat$_x$[M(DDDT)$_2$]^x (XXIII)–(XXIX) (Table 4) and BEDT–TTF (one of the most promising donors in organic conductors). The close similarity between the molecular packing in crystals of BEDT–TTF and Au(DDDT)$_2$ has also been noted.[81]

Crystals of the neutral complexes Ni(DDDT)$_2$ (XXIII) and Au(DDDT)$_2$ (XXVIII) are not isostructural. The crystal of (XXIII) is composed of two symmetrically independent centrosymmetric molecules. In both molecules the lengths of the formally double C=C bonds [1.389 and 1.388(4) Å] are considerably greater than the length of a normal C=C double bond (in cyclopentene, for example, r(C=C) = 1.323 Å),[85] approaching the length of a C ⩬ C aromatic bond (1.380 Å).[85] Electron delocalisation in the chelate residues (Ni)S ⩬ C ⩬ C ⩬ S(Ni), in the same way as in M(dmit)$_2$ complexes, may be assumed to occur in this case. It may also be assumed[36,79] that there is an approximately equal contribution of both canonical forms of the ligands (Scheme 1) to the valence state of DDDT. The average charge of each ligand is equal to -1, and the electronic configuration of the Ni atom (occurring in a formal oxidation state of 2+) is d^8.

Scheme 1



Complex (XXIII) has an essentially planar structure, the maximum deviation (Δ_{max}) of the atoms (without taking into account the peripheral C atoms of the ligands) from the plane of the central NiS_4 residue does not exceed 0.03(1) Å. Amongst the M(DDDT)$_2$ complexes in (XXIII)–(XXIX) the greatest deviation from planarity occurs in the neutral complex (XXVIII) [Δ_{max} = 0.77(1) Å]. On the whole M(DDDT)$_2$ complexes are less rigid and more likely to undergo distortion of the planar structure than M(dmit)$_2$ complexes.

In the crystal of (XXIII) two independent $Ni(DDDT)_2$ molecules are arranged in separate stacks along the short *b* translation. The angles formed by the normals to the coordination planes of the Ni atoms in the molecules of (XXIII, A) and (XXIII, B) with the *b* axis are similar (36.1 and 36.7°). The interplanar distances in the stacks of molecules (XXIII, A) and (XXIII, B) are equal to 3.78 and 3.75 Å. There are no shortened S...S contacts within the stacks. On the other hand, shortened S...S contacts occur between the stacks [3.594(3) and 3.483(3) Å].

The Ni–S distances in the $[Ni(DDDT)_2]^-$ anions of salts (XXIV) [2.146 and 2.149(2) Å] and (XXV) [2.130–2.145(9) Å] are slightly greater than in the neutral $Ni(DDDT)_2$ complex (XXIII) [2.129–2.135(1) Å]. A similar trend was noted above for complexes of the type $[M(dmit)_2]^x$. In the crystal of (XXIV) anions form layers and cations are arranged between these layers. The S...S distances in the crystal of (XXIV) are not reduced. In the crystal of (XXV) there are two types of symmetrically independent anion—(XXV, A) and (XXV, B). Anions (XXV, A) form stacks (with partial overlap of the orbitals of the anions) along the *a* axis, anions (XXV, B) are arranged roughly perpendicular to anions (XXV, A) and do not form stacks (Fig. 20). As in (XXIV), there are no shortened intermolecular S...S contacts in the structure of (XXV).

Crystals of the salt $(Bu_4N)[Ni(DDT)_2]$ (XXVI), which differs from (XXV) in that unsaturated ethylene residues occur in the DDT ligands instead of saturated residues in the DDDT ligands, are composed, in the same way as crystals of (XXV), of two symmetrically independent centrosymmetric anions (XXVI, A) and (XXVI, B). All of the atoms in the anions lie in the same plane, with the exception of the terminal C atoms of the peripheral rings. Thus, the 1,4-dithiin rings are bent along the line of S...S by 28.2° [anion (XXVI, A)] and 38.8° [anion (XXVI, B)]. Anions (XXVI, B), overlapping in a displaced manner, form stacks along the *b* axis with an interplanar distance of $d = 4.03$ Å. Anions (XXVI, A) do not form stacks, but, alternating with cations, are aligned into layers, parallel to *bc*.

Kim et al.[86] have discussed the results of an EH calculation of the coefficients of the real part of the expression for the LUMOs of the $[Ni(DDT)_2]^-$ anion, which have the same symmetry as the LUMOs of the $[Ni(dmit)_2]^-$ and $[Ni(DDDT)_2]^-$ anions.[86] In the case of the $[Ni(dmit)_2]^-$ anion, the contribution of the LUMOs localised on the "outer" $S(a_0)$ atoms constitutes about 1/5 of the contribution (a_i) of the "inner" S atoms (bonded to the Ni atom), therefore the interaction between the "terminal" molecules in crystals of $Ni(dmit)_2$ complexes is small.[87] In the $[Ni(DDDT)_2]^-$ anion there is the relationship $a_0/a_i \approx 1/2$, which must favour the formation of two-dimensional electroconductive motifs. In the $[Ni(DDT)_2]^-$ anion the relationship $a_0/a_i \approx 3/5$ is even more favourable for the formation of two-dimensional motifs; however, as has been noted,[81] in the synthesis of organic metals an important factor is the

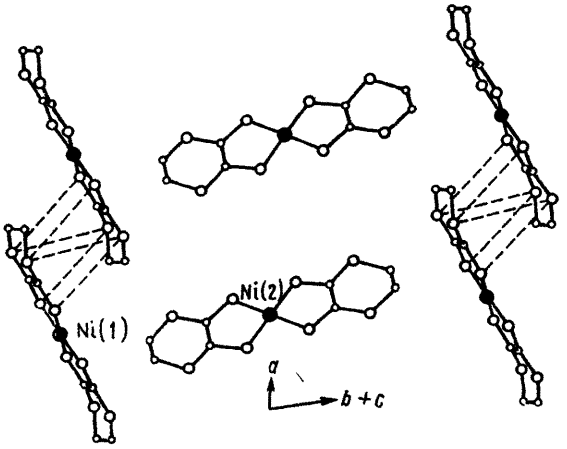


Figure 20. Packing of $[Ni(DDDT)_2]^-$ anions in the crystal of (XXV). The (XXV, A) anions [Ni(1) atom] form stacks (with partial overlap of the anions along the *a* axis). The S...S contacts in the stacks (depicted by broken lines) are not shortened. The (XXV, B) anions [Ni(2) atom] are arranged roughly perpendicular to the (XXV, A) stacks.[82]

Table 4. The main data on $[M(DDDT)_2]^x$ and $[M(DDT)_2]^x$ compounds.

Compound	Chemical formula	*x*	M–S distance, Å	Main structural motif	Conductivity σ_{293}, Ω^{-1} cm^{-1}	Refs.
(XXIII)	$Ni(DDDT)_2$	0	2.129–2.135(1)	Stacks (d=3.75 and 3.78 Å)	10^{-5}–10^{-6}	[79, 80]
(XXIV)	$(Et_4N)[Ni(DDDT)_2]$	–1	2.146; 2.149(2)	Layers	see*	[81]
(XXV)	$(Bu_4N)[Ni(DDDT)_2]$	–1	2.130–2.145(9)	Stacks of (XXV, A) anions	see*	[82]
(XXVI)	$(Bu_4N)[Ni(DDT)_2]$	–1	2.129–2.149(10)	Stacks of (XXVI, B) anions	see*	[83]
(XXVII)	$[Ni(DDDT)_2]_3(ClO_4)_2$	2/3	2.1593–2.1720(1)	Trimers→stacks→layers	see*	[80, 84]
(XXVIII)	$Au(DDDT)_2$	0	2.280–2.317(9)	Dimers→three-dimensional structure	~10^{-4}	[82]
(XXIX)	$(Et_4N)[Au(DDDT)_2]$	–1	2.310; 2.312(3)	Not formed	10^{-5}–10^{-6}	[79]

*No accurate conductivity values.

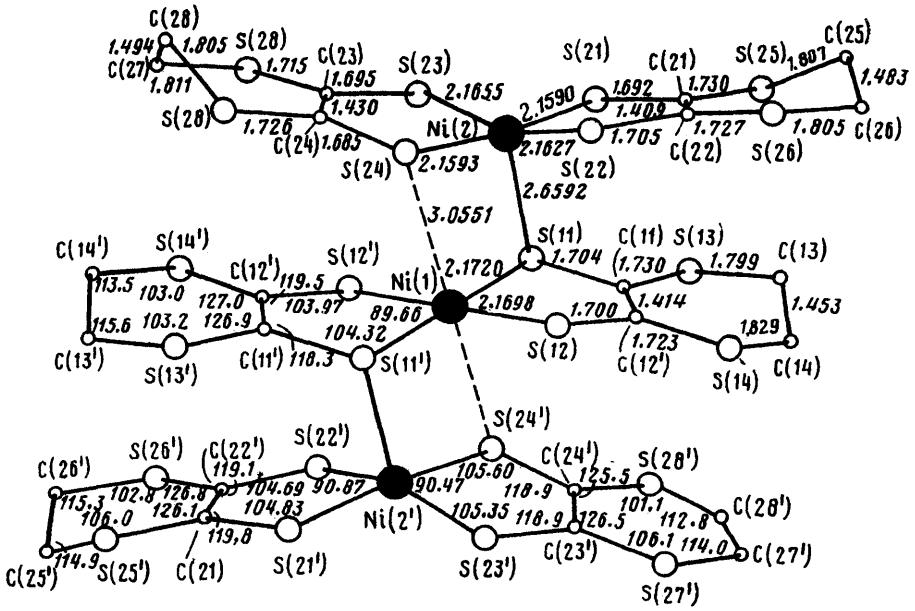


Figure 21. Structure of the trimeric $[Ni(DDDT)_2]_3^{2+}$ cation in the crystal of (XXVII).[80,84]

electrochemical properties of the components,§ namely, the magnitude of $\Delta E = E_1 - E_2$, which for the $[Ni(DDT)_2]^-$ anion has a value intermediate between ΔE for the $[Ni(dmit)_2]^-$ and $[Ni(DDDT)_2]^-$ anions.

The formal degrees of oxidation of the Ni atom and DDDT ligand in the $[Ni(DDDT)_2]^-$ complex can be represented as $[Ni^{3+}(d^7)(DDDT)_2^{2-}]^-$ or $[Ni^{2+}(d^8)(DDDT)_2^{3-}]^-$. For d^7 and d^8 configurations of the Ni atom the unpaired electron is situated on the metal atom or DDDT ligand respectively. The d^8 configuration is more consistent with a square planar coordination of the metal atom. Calculations of the population of the atomic orbitals of the Ni atom in the $[Ni(DDDT)_2]^-$ atom as well as magnetic measurements confirm a d^8 configuration of the Ni atom in this salt and that the unpaired electron is mainly located on the DDDT ligands.[82]

Salt (XXV) is paramagnetic over the whole temperature range of magnetic susceptibility measurements (from 300 to 4.2 K) in contrast to salt (XXIV), which is characterised by ferromagnetic exchange below 15 K. This difference between salts (XXIV) and (XXV) is probably due to the larger size of the cations in (XXV), which leads to an increase in intermolecular S...S distances, resulting in a weakening of magnetic exchange.[82] In fact, the shortest intermolecular S...S distances in the crystal of (XXIV) (3.98 Å within layers and 4.49 Å between layers) is appreciably less than in the crystal of (XXV) (4.75 Å within the stacks).

Electrochemical oxidation of complex (XXIII) gives salt (XXVII), the crystal of which is composed of the centrosymmetric trimeric cations $[Ni(DDDT)_2]_3^{2+}$ and two symmetrically independent ClO_4^- anions occurring in general positions. This cationic structure of the $[Ni(DDDT)_2]_3^{2+}$ complex is quite surprising. In the other crystals of (XXIII)–(XXIX) (Table 4) the $[M(DDDT)_2]^x$ complexes occur either in anionic or neutral forms. Amongst related $[M(dmit)_2]^x$ complexes that have been sufficiently well studied (in relation to the structure and electrical conductivity), again only anionic and neutral complexes are known.

The structures of the inner and outer residues of the trimeric cation of (XXVII) are considerably different. The central Ni(1) atom has a square planar coordination, increased to a [4+2]-type of pseudo-octahedral coordination through Ni(1)...S(24) and Ni(1)...S(24') interactions [3.0551(6) Å] (Fig. 21). The Ni(1)...S(24) vector forms an angle of 86.5° with the S(11)S(12)S(11')S(12') equatorial coordination plane of the Ni(1) atom. The Ni(2) atom [and symmetrically equivalent Ni(2') atom] has a fivefold tetragonal pyramidal coordination and deviates by 0.291 Å from the basal S(21)S(22)S(23)S(24) plane towards the apical S(11) atom of the inner cation residue. The basal Ni(2)–S distance [2.1590–2.1655(6) Å] is somewhat less than the equatorial Ni(1)–S distances [2.1698 and 2.1720(6) Å] and is appreciably less than the apical Ni(2)–S(11) distance [2.6592(7) Å]. All of the basal Ni–S distances in the cation of (XXVII) are clearly greater than in the neutral complex (XXIII) and anions of (XXIV) and (XXV).

The considerable similarity between the lengths of the corresponding S–C and C–C bonds in the inner and outer DDDT ligands of complex (XXVII) should be noted (Fig. 21). On the whole the lengths of the C–C bonds (average 1.418 Å) and S–C (average 1.697 Å) suggest that, as in complex (XXIII), there is appreciable delocalisation of electron density in the chelate rings and that there is an approximately equal contribution of the two canonical forms (*a*) and (*b*) (Scheme 1) to the state of the ligands of DDDT. The cation of (XXVII) can be represented as $\{[Ni^{2+}(d^8)(DDDT^-)_2][Ni^{3+}(d^7)(DDDT^-)_2]_2\}$.[80,84]

The association of dithiolene complexes through M...S interactions is well-known.[36] However, only dimeric dithiolate complexes with a coordination of the M atom of the type [4+1]

§ E_1 and E_2 are the values of the redox potentials for the reactions $[ML_2]^2 \overset{E_1}{\rightleftarrows} [ML_2]^- \overset{E_2}{\rightleftarrows} [ML_2]^0$, where ML_2 is the 1,4-dithiolene complex of the metal.[88]

were previously studied structurally.[36] Thus, the Fe atoms in the centrosymmetric dimer $\{Fe_2[S_2C_2(COOMe)_2]_4\}^{2-}$ formed through Fe...S interactions [Fe–S_{bas} distances equal to 2.230–2.256(2) Å, Fe–S_{apic} distance is 2.446(2) Å, projection of the Fe atoms from the basal planes $\Delta(Fe_{bas})$ = 0.434(1) Å, Fe...Fe is 3.120 Å] have [4+1] coordination similar to the Ni(2) atom.[89] Polymeric dithiolene complexes with a [4+2]-type of coordination of the Ni atoms (Fig. 22), like the Ni(1) atom in (XXVII), have also been theoretically predicted.[36] However, such structures have so far not been detected experimentally.

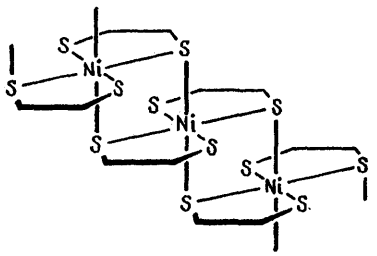


Figure 22. Hypothetical polymer chain of $Ni(edt)_2$ complexes (edt = ethylenedithiolate) combined through Ni...S interactions with [4+2] coordination of the Ni atoms.[36]

Despite the eclipsed relative configuration of the central and outer residues (Figs. 21 and 23), there is no substantial steric strain in the cation of (XXVII). The intercation contacts between the inner and outer residues [S(11)...S(23) 3.676(3) Å, S(11)...S(24′) 3.694(3) Å, S(12)...S(24′) 3.652(3) Å] are only slightly less than twice the van der Waals radius of the S atom (3.70 Å).[80] The Ni(1)...Ni(2) distance is 3.3310(4) Å, i.e., it does not correspond to a metal–metal interaction.

The cations in the crystal of (XXVII) are arranged in stacks along the axis c = 12.148 Å (Fig. 23). The S...S contacts in the stacks between the trimers are not shortened. Shortened contacts occur between stacks: $S(11)...S(25)_A$ 3.667(3) Å, $S(12)...S(21)_D$ 3.606(3) Å, $S(12)...S(26)_B$ 3.657(3) Å, $S(13)...S(25)_A$ 3.366(3) Å, $S(21)...S(24)_E$, 3.609(3) Å, $S(22)...S(23)_D$ 3.547(3) Å, $S(23)...S(26)_E$ 3.463(3) Å, $S(26)...S(27)_D$ 3.514(3) Å [atom S_A is projected from the S atom by the transformation $(x, \frac{1}{2}-y, \frac{1}{2}+z)$, S_B by $(x, 3/2-y, \frac{1}{2}+z)$, S_E by $(-x, -\frac{1}{2}+y, \frac{1}{2}-z)$, and S_D by $(-x, \frac{1}{2}+y, \frac{1}{2}-z)$]. These shortened contacts combine the stacks of cations into layers, parallel to the *bc* plane of the crystal of (XXVII).

The molecular metal $(BEDT-TTF)_3(ClO_4)_2$ has a structure very similar to (XXVII); there are stacks along the [011] direction, in which triads of BEDT–TTF radical cations are separated with a period of 12.172 Å, short S...S contacts occurring only between stacks.[90] The low electrical conductivity of (XXVII) is probably due to the high localisation of charges in the cation trimers.

$Au(DDDT)_2$ complexes (XXVIII) are packed in the crystal with the same structural motif (centrosymmetric dimers) as for neutral BEDT–TTF molecules (Fig. 24). The similarity of structural motifs with comparable parameters of the unit cells [(XXVIII): a = 6.496(1) Å, b = 13.267(4) Å, c = 16.775(3) Å, β = 94.87(2)°, V = 1440.5(5) Å^3, Z = 4, space group $P2_1/n$; BEDT–TTF (transformed cell):[82] a = 6.614 Å, b = 13.985 Å, c = 15.721 Å,

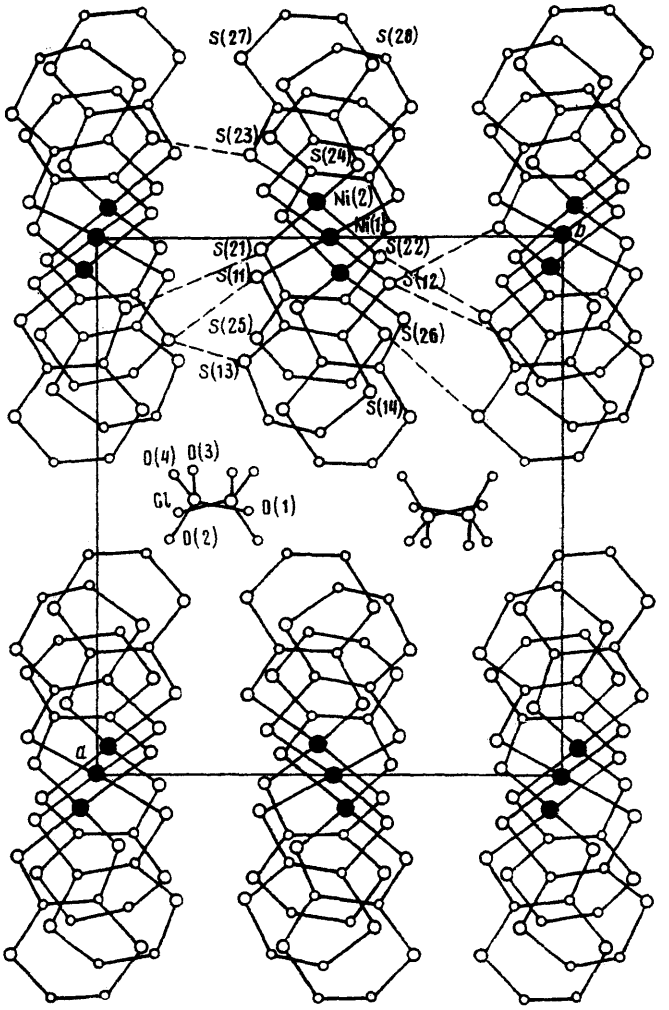


Figure 23. Projection of the crystalline structure of (XXVII) on to the *ab* plane. Shortened intercation S...S contacts are indicated by broken lines.[80,84]

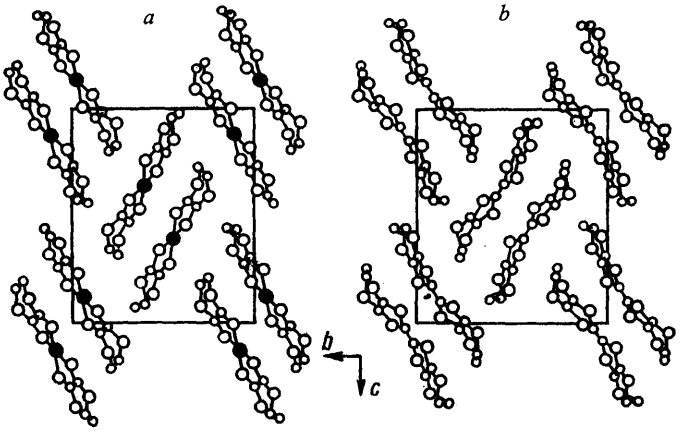


Figure 24. Projections of the crystalline structures of (XXVIII) (*a*) and BEDT–TTF (*b*) on to the *bc* plane. The diagram is taken from the study of Schultz et al.[82] and converted to the modified coordinates given by Kobayashi et al.[91]

$\beta = 93.81°$, $V = 1451$ Å^3, $Z = 4$, space group $P2_1/n$] is consistent with the structural similarity of the (XXVIII) and BEDT–TTF molecules. Shortened intermolecular S...S contacts (<3.70 Å) in both crystals only occur between dimers and combine the molecules into a three-dimensional system, and judging by the values of these contacts [the two crystals each have five shortened contacts: 3.59–3.67 Å in (XXVIII) and 3.48–3.69 Å in BEDT–TTF], the packing of the BEDT–TTF molecules is denser.

The Au–S distance in the $[Au(DDDT)_2]^-$ anion in the crystal of (XXIX) [2.310 and 2.312(3) Å (average 2.311 Å)] is slightly greater than in the neutral $Au(DDDT)_2$ complex (XXVIII) [2.280–2.317(9) Å (average 2.304 Å)] and is in good agreement with those found in $[Au(dmit)_2]^{n-}$ anionic complexes (see Table 2). It is not possible to make any definite conclusions as to whether there is electron delocalisation because of the insufficient accuracy of the X-ray diffraction study of compound (XXIX). Significant structural motifs in terms of electrical conductivity (stacks, layers) are absent and there are no shortened interanion S...S contacts.

Let us consider one more ligand system containing a tetrathioethylene unit, namely, 5,6-dihydro-1,4-dithiepin-2,3-dithiolate (DDTDT). Metal complexes obtained from it are structurally similar to the BEDT–TTF molecule. The presence of the "extra" methylene unit in this ligand (compared to the DDDT ligand) results in an even greater deviation from planarity in DDTDT ligands, namely, in a further weakening of the intrastack interaction in crystals of $[M(DDTDT)_2]^x$ complexes relative to the interstack interaction. The main data on the structure of $[M(DDTDT)_2]^x$ complexes are given in Table 5.

Table 5. The main data on the structure of $[M(DDTDT)_2]^x$ complexes.[92]

Compound	Chemical formula	x	M–S distance, Å	Main structural motif	Conductivity σ_{293}, Ω^{-1} cm^{-1}
(XXX)	$Ni(DDTDT)_2$	0	2.121, 2.138 (1)	Stacks	10^{-6}
(XXXI)	$(Et_4N)[Ni(DDTDT)_2]$	−1	2.139–2.151 (1)	Chains	10^{-5}
(XXXII)	$(Et_4N)[Cu(DDTDT)_2]$	−1	2.179–2.190 (1)	"	10^{-6}

In the crystal of (XXX) the neutral $Ni(DDTDT)_2$ complexes occupy specific positions on the 2 axes, forming stacks along the z axis ($c = 7.553$ Å). The Ni...Ni distance (3.777 Å) in a stack is too long for a metal–metal bond to be formed; there are no shortened S...S contacts in the crystal of (XXX). The central residue of complex (XXX) (excluding the C atoms of the trimethylene groups) is virtually planar ($\Delta_{max} = 0.083$ Å).

The $[Ni(DDTDT)_2]^-$ and $[Cu(DDTDT)_2]^-$ anions in the isostructural salts (XXXI) and (XXXII) have the same, almost planar structure [$\Delta_{max} = 0.088$ and 0.053 Å in the two symmetrically independent centrosymmetric anions in the crystal of (XXXI) and 0.068 and 0.072 Å in the crystal of (XXXII)]. The Ni–S distances in the $[Ni(DDTDT)_2]$ anion [2.139–2.151(1) Å] are slightly greater than in the neutral $Ni(DDTDT)_2$ complex [2.121 and 2.138(1) Å]. The anions in the crystals of (XXXI) and (XXXII) are combined into short chains along the [101] direction through short S...S contacts between the outer S atoms of the ligands [3.505 Å in (XXXI) and 3.519 Å in (XXXII)]. A stack structure does not occur in the crystals of (XXXI) and (XXXII).

V. Conclusion

By studying the structure of complexes of the type $[M(dmit)_2]^x$ and $[M(DDDT)_2]^x$ it was possible to obtain new information about the composition of low-dimensional molecular conductors. It was found at the same time that while the crystalline structure of salts of the type $(Me_4N)_{0.5}[Ni(dmit)_2]$ [(II), $\sigma = 50$ Ω^{-1} cm^{-1}] with organic cations of small size is very much like the structure of the previously known alkali metal dithiolates of the type $Li_{0.82}\{Pt[S_2C_2(CN)_2]\}\cdot 2H_2O$ with relatively good conductivity ($\sigma = 10^2$ Ω^{-1} cm^{-1},[59] fairly dense, regular, or slightly dimerised stacks of anions combined into layers), the structural motifs of crystals of $(Bu_4N)_{0.29}[Ni(dmit)_2]$ [(V), $\sigma = 1–10$ Ω^{-1} cm^{-1}, alternation of triads and tetrads in stacks of anions] and $(Ph_4As)_{0.25}[Ni(dmit)_2]$ [(VIII), $\sigma = 10–15$ Ω^{-1} cm^{-1}, tetrads in anion stacks] are very unusual. The structure of the crystal of $(Me_3S)[Au(dmit)_2]$ [(XIII), $\sigma = 10^{-5}$ Ω^{-1} cm^{-1}], which has a well-defined layer structure, the layers being formed by both anions and cations, is also unusual. It should also be noted that the structure of the anion stacks characteristic of the salts $(Me_4N)_{0.5}[Ni(dmit)_2]$ (II), $(Et_4N)_{0.5}[Ni(dmit)_2]$ (III), and α-$\{(Et_4N)_{0.5}[Au(dmit)_2]\}$ (X), which have relatively good conductivity, also occurs in their nonconductive precursors, such as in $(Et_4N)[Au(dmit)_2]$ (XI). It is true that in the latter case the stacks are not combined into layers.

Segregated stacks of donors and acceptors constitute the predominant structural motif in the highly conductive salts $D[M(dmit)_2]_x$ (D = open donor), such as $(TTF)[Ni(dmit)_2]_2$ [(XV), $\sigma = 300$ Ω^{-1} cm^{-1}], which was found previously in salts of dithiolate complexes with organic donors, such as $(C_{20}H_{12})_2\{Pt[S_2C_2(CN)_2]_2\}$, where $C_{20}H_{12}$ = perylene ($\sigma = 400$ Ω^{-1} cm^{-1})[93] and would appear to be the most conducive to a high electrical conductivity.

The structure of $(HMTTeF)[Pt(dmit)_2]_{0.5}$ [(XXII), $\sigma = 20$ Ω^{-1} cm^{-1}] is unusual. The crystal of (XXII) comprises layers of tetrads of donor molecules, the acceptor molecules being perpendicular to these layers. Quite unexpected was the comparatively high electrical conductivity of the salt (BEDT–TTF)[Ni(dmit)$_2$] [(XIX), $\sigma = 0.02$ Ω^{-1} cm^{-1}]. The crystal of (XIX) is composed of stacks with a different structure. A quantum-chemical calculation of the zone structure showed that the electrical conductivity of this salt is caused by "lateral" donor–donor (primarily) and acceptor–acceptor interactions.

Amongst these structures are to be found two forms of association of dithiolate complexes, discussed in detail by Alvarez et al.[36] In the crystal of $(TTF)[Pt(dmit)_2]_3$ [(XXI), $\sigma = 20$ Ω^{-1} cm^{-1}], one of the symmetrically independent anions participates in the formation of dimers through a direct Pt–Pt bond, whereas the second anion remains in monomer form, the acceptor stacks (combined into electroconductive layers) are composed of alternating dimers.

The second possible form of association of dithiolene complexes occurs in the crystal of $[Ni(DDDT)_2]_3(ClO_4)_2$, (XXVII), in whose trimeric dication the Ni atoms have different types of coordination. The outer atoms have a square pyramidal coordination (through a direct Ni–S bond with the inner residue), the inner atom has a pseudo-octahedral [4+2] coordination (through additional Ni...S interactions with the outer residues).

The sixfold coordination¶ of the inner Ni atom is an indication of the possible formation of infinite one-dimensional motifs of $[M(DDDT)_2]$ complexes. A further feature of the crystal of $[Ni(DDDT)_2]_3(ClO_4)_2$ is that it is essentially isostructural with the $(BEDT-TTF)_3(ClO_4)_2$ crystal, in which triads of BEDT–TTF radical cations (also arranged in stacks) act as a structural analogue of the trimeric cations (arranged in stacks). It is known that $(BEDT-TTF)_3(ClO_4)_2$ exhibits superconductive properties at very low temperatures.

Of the dithiolates discussed in this review, only crystals of $(Me_4N)_{0.5}[Ni(dmit)_2]$ (II) and $(TTF)[Ni(dmit)_2]_2$ (XV) undergo a transition to a superconductive state. Although the complex $[Ni(DDDT)_2]_3(ClO_4)_2$ (XXVII) has low electrical conductivity and is a semiconductor, its close structural similarity to $(BEDT-TTF)_3(ClO_4)_2$ gives grounds for the hope that replacement of ClO_4^- by other anions (differing from ClO_4^- in size, shape, and charge) and of Ni by another complex-forming metal (Pt, Pd, Cu) may lead to the formation of highly conductive compounds based on monomeric or polymeric $[M(DDDT)_2]^x$ complexes as donors.

On the whole, dithiolate complexes of transition metals now form an important independent class of molecular conductors (although this has much in common with purely organic conductors). There are many opportunities for modifying the structure and properties of the dithiolates. There is greatest interest in the transition from isolated monomeric dithiolates to one-dimensional and particularly two-dimensional structural motifs, namely, approaching the structures and essentially two-dimensional properties such as those of high-temperature inorganic superconductors.

References

1. V E Shklover, T V Timofeeva, Yu T Struchkov *Usp. Khim.*, 1986, **55**(8) 1282 [English translation in *Russ. Chem. Rev.*, 1986(8)]
2. V E Shklover, T V Timofeeva *Usp. Khim.*, 1985, **54**(7) 1057 [English translation in *Russ. Chem. Rev.*, 1985(7)]
3. E Weber *Molecular Inclusion and Molecular Recognition. Clathrates. I. Top. Curr. Chem.*, 1987, **140** 3
4. C N R Rao, J Gopalakrishnan *New Directions in Solid State Chemistry*, 1986, p. 637
5. H Seki, T Uchida, Y Shibata *Mol. Cryst. Liq. Cryst.*, 1986, **138** 349
6. J S Miller, A J Epstein, W M Reiff *Chem. Rev.*, 1988, **88** 201
7. G R Desiraju *Prog. Solid State Chem.*, 1987, **17** 295
8. X Sishen, S Geller *J. Solid State Chem.*, 1987, **68** 73
9. H Eckhardt, G G Miller, R H Baughman *Synth. Met.*, 1984, **9** 441
10. R E Dickerson, M L Kopka, P Pjura *Chem. Scr. B*, 1986, **26** 139
11. C R Thocharis, W Jones, C N R Rao *J. Chem. Soc., Chem. Commun.*, 1984, 1291
12. L J W Shimon, M Lahav, L Leiserowitz *Nouv. J. Chim.*, 1986, **10** 723
13. Yu E Ovchinnikov, V E Shklover, Yu T Struchkov, et al. *Makromol. Chem.*, 1988, **189** 1927
14. R Schollhorn *Inclusion Compounds*, 1984, **1** 249
15. Yu E Ovchinnikov. V E Shklover, Yu T Struchkov *Dokl. Akad. Nauk SSSR*, 1987, **295** 914
16. D J Sandman, B S Elman, G P Hamill, et al. *Mol. Cryst. Liq. Cryst. Lett.*, 1987, **4** 77
17. R L Greene, G B Street *Science*, 1984, **226** 651
18. E B Yagubskii, P F Shchegolev, V N Topnikov, et al. *Zh. Eksp. Teor. Fiz.*, 1985, **88** 244
19. I F Shchegolev *Phys. Status Solidi. A*, 1972, **12** 9
20. R P Shibaeva *Kristallokhimiya* (Crystal Chemistry), Izd. VINITI, Moscow, 1981, Vol. 15, p. 189 (Advances in Science and Technology)
21. D Jerome, A Mazaud, M Ribault, K Bechgaard *J. Phys. Lett.*, 1980, **41** L195
22. J M Williams, M A Beno, H H Wang, et al. *Acc. Chem. Res.*, 1985, **18** 261
23. N Thorup, G Rindorf, H Soling, et al. *J. Phys. (France)*, 1983, **44** 3, Suppl. 6, 3–1017
24. B Gallois, J Gaultier, C Hauw, T Lamcharfi *Acta Crystallogr., Sect. B*, 1986, **42** 564
25. G Saito, T Enoki, K Toriumi, H Inokuchi *Solid State Commun.*, 1982, **42** 557
26. R P Shibaeva, V F Kaminskii, E B Yagubskii *Mol. Cryst. Liq. Cryst.* 1985, **119** 361
27. P C W Leung, T J Emge, M A Beno, et al. *J. Am. Chem. Soc.*, 1985, **107** 6184
28. K Bechgaard, D Jerome *Usp. Fiz. Khim.*, 1983, **140** 671
29. E B Yagubskii, I F Shchegolev, R P Shibaeva *Pis'ma Zh. Eksp. Teor. Fiz.*, 1985, **42** 167
30. H Urayama, H Yamouchi, G Saito, et al. *Chem. Lett.*, 1988, 463
31. K D Carlson, U Gieser, A M Kini, et al. *Inorg. Chem.*, 1988, **27** 965
32. D Schweitzer, I Hennig, K Bender, et al. *Mol. Cryst. Liq. Cryst.*, 1985, **120** 213
33. Z G Soos, H J Keller *Chemistry and Physics of One-Dimensional Metals* (Edited by H J Keller), Plenum Press, New York, NATO-ASI Series B25, 1977, p. 391
34. H J Keller, R Niebl, D Nothe, et al. *Physica B*, 1985, **143B** 301
35. P Kuppusamy, A Ramakrishna, P T Monaharan *Proc. Indian Acad. Sci., Chem. Sci.*, 1984, **93** 977
36. S Alvarez, R Vicente, R Hoffman *J. Am. Chem. Soc.*, 1985, **107** 6253
37. L Valade, J-P Legros, M Bousseau, et al. *J. Chem. Soc., Dalton Trans.*, 1985, 783
38. H Kim, A Kobayashi, E Sasaki, et al. *Chem. Lett.*, 1987, 1799
39. A Kobayashi, H Kim, Y Sasaki, et al *Chem. Lett.*, 1987, 1819
40. R Kato, H Kobayashi, H Kim, et al. *Chem. Lett.*, 1988, 865
41. R Kato, T Mori, A Kobayashi, et al. *Chem. Lett.*, 1984, 1
42. L Valade, M Bousseau, A Gleizes, P Cassoux *J. Chem. Soc., Chem. Commun.*, 1983, 110
43. O Lindqist, L Sjolin, J Sieler, et al. *Acta Chem. Scand., Ser. A*, 1979, **33** 445
44. S S Nagapetyan, V E Shklover, Yu T Struchkov, et al. *Zh. Neorg. Khim.*, (at the press)
45. L Valade, J-P Legros, P Cassoux, F Kubel *Mol. Cryst. Liq. Cryst.*, 1986, **140** 335
46. V A Starodub, V N Baumer, M A Obolenskii *Koord. Khim.*, 1987, **13** 1403

¶Data exist[94] on the formation of one-dimensional and other motifs through [4+2] coordination of Ni atoms, such as the ...I...$[Ni_2S_8]$...I...$[Ni_2S_8]$... chains in the structure of $[Ni(CH_2CS_2)_2]_2I$ [Ni–Ni distance in the dimer 2.514(3) Å, Ni...I 2.928 and 2.940(4) Å].

47. S S Nagapetyan, V E Shklover, A I Kotov, et al. *Mater. Sci.*, (at the press)
48. E B Yagubskii, L Yu Ukhin, V E Shklover, et al. *Dokl. Akad. Nauk SSSR*, 1986, **290** 115
49. A A Macharashvili, L V Belousova, Z S Morkovnik, et al. *Zh. Neorg. Khim.*, 1987, **32**(8) 1897 [English translation in *Russ. J. Inorg. Chem.*, 1987(8)]
50. S S Nagapetyan, E R Arakelova, L V Belousova, et al. *Zh. Neorg. Khim.*, 1988, **33**(1) 160 [English translation in *Russ. J. Inorg. Chem.*, 1988(1)]
51. L Pauling *The Nature of the Chemical Bond* (3rd Edition), Cornell Univ. Press, Ithaca–New York, 1960, p. 644
52. J Simon, F Tournilhac, J-J Andre *Nouv. J. Chim.*, 1987, **11** 383
53. T Mori, A Kobayashi, Y Sasaki, et al. *Bull. Chem. Soc. Jpn.*, 1984, **57** 627
54. D Jerome *Mol. Cryst. Liq. Cryst.*, 1982, **79** 155
55. M Tokumoto, H Bando, K Murata, et al. *Synth. Met.*, 1985, **13** 9
56. A Kobayashi, H Kim, Y Sasaki, et al. *Solid State Commun.*, 1987 **62** 57
57. M Bousseau, L Valade, M-F Breuriquel, P Cassaux *Nouv. J. Chim.*, 1984, **8** 3
58. M Bousseau, L Valade, J-P Legros, et al. *J. Am. Chem. Soc.*, 1986, **108** 1908
59. A Kobayashi, Y Sasaki, H Kobayashi, et al. *J. Chem. Soc., Chem. Commun.*, 1982, 390
60. C Mahedavan *J. Cryst. Spectrosc. Res.*, 1986, **16** 159
61. I Johannsen, K Bechgaard, G Rindorf, et al. *Synth. Met.*, 1986, **15** 333
62. H Kobayashi, R Kato, A Kobayashi, Y Sasaki *Chem. Lett.*, 1985, 535
63. R Kato, H Kobayashi, A Kobayashi, Y Sasaki *Chem. Lett.*, 1985, 131
64. H Kobayashi, R Kato, A Kobayashi, Y Sasaki *Chem. Lett.*, 1985, 191
65. A Kobayashi, R Kato, H Kobayashi *Synth. Met.*, 1987, **19** 635
66. A Kobayashi, Y Sasaki, R Kato, H Kobayashi *Chem. Lett.*, 1986, 387
67. G Rindorf, H Soling, N Thourp *Acta Crystallogr., Sect. B*, 1982, **38** 2805
68. T Mori, A Kobayashi, Y Sasaki, H Kobayashi *Chem. Lett.*, 1982, 1923
69. S Shitzkowsky, M Weger, H Gutfrennd *J. Phys. (Paris)*, 1978, **39** 711
70. U Bernstein, P M Chaikin, P Pincus *Phys. Rev. Lett.*, 1975, **34** 271
71. T Mori, R Kobayashi, Y Sasaki, et al. *Bull. Chem. Soc. Jpn.*, 1984, **57** 627
72. T Mori, A Kobayashi, Y Sasaki, et al. *Chem. Lett.*, 1984, 957
73. K W Borwall, T Bursch, L V Interrante, J S Kasper *Inorg. Chem.*, 1972, **11** 1800
74. K Kikuchi, K Yakuchi, H Kuroda, et al. *Chem. Lett.*, 1985, 419
75. R Kato, H Kobayashi, T Mori, et al. *Solid State Commun.*, 1985, **55** 387
76. L Brossard, M Ribault, M Bousseau, et al. *C.R. Seances Acad. Sci.*, 1986, **302** 205
77. J S Miller *Extended Linear Chain Compounds*, Plenum Press, New York, 1982, Vol. 1, 2; 1983, Vol. 3
78. F Wudl *Pure Appl. Chem.*, 1982, **54** 1051
79. S S Nagapetyan, L V Vetoshkina, A I Kotov, et al. *Zh. Neorg. Khim.*, (at the press)
80. S S Nagapetyan, V E Shklover, Yu T Struchkov, et al. *Mater. Sci.*, 1988, **14** 5
81. C T Vance, R D Bereman, I Bordner, et al. *Inorg. Chem.*, 1985, **24** 2905
82. A J Schultz, H H Wang, L C Soderholm, et al. *Inorg. Chem.*, 1987, **26** 3757
83. H Kim, A Kobayashi, Y Sasaki, et al. *Bull. Chem. Soc. Jpn.*, 1988, **61** 2559
84. S S Nagapetyan, V E Shklover, Yu T Struchkov, et al. *Dokl. Akad. Nauk SSSR*, 1990, **310** 94
85. F H Allen, O Kennard, D G Watson, et al. *J. Chem. Soc., Perkin Trans. 2*, 1987, S1
86. H Kim, A Kobayashi, Y Sasaki, et al. *Bull. Chem. Soc. Jpn.*, 1988, **61** 579
87. A Kobayashi, H Kim, Y Sasaki, et al. *Solid State Commun.*, 1987, **67** 57
88. T Nakamura, T Nogami, Y Shirota *Bull. Chem. Soc. Jpn.*, 1987, **60** 3447
89. M G Kanatzidis, D Coucouvanis *Inorg. Chem.*, 1984, **23** 403
90. H Kobayashi, R Kato, T Mori, et al. *Chem. Lett.*, 1984, 179
91. H Kobayashi, A Kobayashi, Y Sasaki, et al. *Bull. Chem. Soc. Jpn.*, 1986, **59** 301
92. S S Nagapetyan, V E Shklover, Yu T Struchkov, et al. *Zh. Neorg. Khim.*, (at the press)
93. L Alcacer, H Navais, F Pedroso, et al. *Solid State Commun.*, 1980, **35** 945
94. C Bellitto, G Dessy, V Fares *Inorg. Chem.*, 1985, **24** 2815